



# STUDY OF THE STABILITY OF A MAGLEV TRAIN

PHY204 Semester 4

May 10, 2025

---

Julia Benhamou  
Jules Frealle  
Clément Rauch  
Benjamin Shu



## CONTENTS

---

<b>1</b>	<b>Introduction</b>	<b>4</b>
1.1	Goals and outline . . . . .	4
1.2	Existing Maglev technologies - similarities and differences . . . . .	5
1.2.1	EMS . . . . .	5
1.2.2	EDS . . . . .	5
<b>2</b>	<b>Theoretical background</b>	<b>7</b>
2.1	EMS . . . . .	7
2.1.1	The magnetic circuit method . . . . .	8
2.1.2	The method of images . . . . .	8
2.1.3	One coil per electromagnet . . . . .	9
2.1.4	Two coils of opposite current per electromagnet . . . . .	9
2.2	EDS . . . . .	11
2.2.1	Model . . . . .	11
2.2.2	Approach . . . . .	12
2.2.3	Computation of the flux and Induced current . . . . .	12
2.2.4	Induced B-field and final expression of U . . . . .	14
<b>3</b>	<b>Numerical simulations</b>	<b>15</b>
3.1	EMS . . . . .	15
3.1.1	The magnetic circuit method . . . . .	15
3.1.2	The method of images: one coil per electromagnet . . . . .	15
3.1.3	The method of images: two coils of opposite current per electromagnet . . . . .	16
3.2	EDS . . . . .	16
3.2.1	Parameters . . . . .	17
3.2.2	Procedure . . . . .	17
<b>4</b>	<b>Results and discussion</b>	<b>18</b>
4.1	EMS . . . . .	18
4.1.1	The magnetic circuit method . . . . .	18
4.1.2	The method of images: one coil per electromagnet . . . . .	19
4.1.3	The method of images: two coils of opposite current per electromagnet . . . . .	20
4.1.4	Summary and further improvements . . . . .	21
4.2	EDS . . . . .	22
4.2.1	Guideway coil current . . . . .	22
4.2.2	Potential energy . . . . .	22
<b>5</b>	<b>Conclusion</b>	<b>24</b>
<b>A</b>	<b>Derivations</b>	<b>25</b>
A.1	EMS . . . . .	25
A.1.1	Derivation of the potential energy stored in the left gap by the magnetic circuit method . . . . .	25

A.1.2	Derivation of the force exerted by one source coil on a target coil in the magnetic dipole approximation . . . . .	26
A.1.3	Derivation of the force exerted by one source coil on a target coil in space . . .	27
A.2	EDS . . . . .	28
A.2.1	Derivation of the flux and current . . . . .	28
A.2.2	Derivation of the magnetic field and potential energy . . . . .	30
<b>B</b>	<b>Simulation code</b>	<b>33</b>
B.1	EMS . . . . .	33
B.1.1	Python code for the simulation using the magnetic circuit method . . . . .	33
B.1.2	Python code for the simulation with one coil per electromagnet using the method of images . . . . .	34
B.1.3	Python code for the simulation with two coils of opposite current per electromagnet using the method of images . . . . .	35
B.2	EDS . . . . .	37
B.2.1	Definition of the parameters . . . . .	37
B.2.2	Defining the time-derivative and current on an 8-coil loop . . . . .	37
B.2.3	Computing the B-field along one slice of the guideway and Potential . . . . .	39
B.2.4	Final plotting . . . . .	41
<b>C</b>	<b>References</b>	<b>43</b>

# 1

## INTRODUCTION

Maglev (magnetic levitation) trains represent a revolutionary advancement in transportation technology, using powerful magnetic forces to levitate and propel trains without any physical contact with the tracks. This innovative concept emerged in the mid-20th century, with initial research dating back to the 1960s. Early prototypes were developed in both Germany and Japan, where extensive experimentation and engineering breakthroughs led to the creation of the first operational maglev systems. In Germany, the Transrapid project was one of the earliest successful implementations, while Japan introduced the SCMaglev, a system that set world speed records. These pioneering efforts laid the foundation for modern maglev trains, which are now seen as a potential solution to many of the limitations faced by conventional rail systems.

One of the most significant advantages of maglev trains lies in their speed. Without the frictional resistance between wheels and tracks, maglev systems can achieve much higher velocities than traditional trains, with some models capable of reaching speeds exceeding 300 miles per hour. This makes maglev trains an ideal mode of transport for long-distance, high-speed travel, reducing journey times and increasing connectivity between major cities. Moreover, the smooth, frictionless operation of maglev trains provides a more comfortable ride for passengers, as there are fewer vibrations and less noise compared to conventional rail systems.

In addition to their speed, maglev trains offer several important transportation and environmental benefits. They are inherently more energy-efficient due to the lack of friction, which reduces the wear and tear on the system and allows for smoother acceleration and deceleration. This makes them more cost-effective in the long run, as maintenance

and operational costs can be lower than those associated with traditional trains. From an environmental perspective, maglev trains are far cleaner than conventional transportation methods. They generate minimal emissions, as they are powered by electricity, and can be integrated with renewable energy sources, making them a crucial element in the shift toward more sustainable urban mobility. Furthermore, the absence of contact between the train and track significantly reduces noise pollution, making maglev systems more suitable for densely populated areas.

In addition to these environmental advantages, maglev trains also reduce road congestion, as they offer a fast and efficient alternative to car travel. This shift to rail-based transportation could help alleviate the environmental impact of traffic, particularly in urban areas, by decreasing the number of vehicles on the road and reducing the associated emissions. As technology continues to improve, the expansion of maglev systems could play a pivotal role in transforming public transportation networks worldwide, offering faster, cleaner, and more sustainable alternatives to existing infrastructure. As such, maglev trains represent not just an innovative transportation solution, but also a vital step toward building a more sustainable future in global mobility.

### 1.1 GOALS AND OUTLINE

The objective of this research project is to understand the mechanisms in place in different Maglev trains to ensure stability of the system. We would like to study the guidance force on the Japanese maglev train, with a focus on understanding the passive stabilization mechanisms that govern the system's stability. As maglev trains rely on magnetic forces for both levitation and guidance, the stability of these vehicles is of paramount importance, especially since they "fly" above the track without physical contact. We aim to develop mathematical models and equations that describe how the magnetic fields interact to provide passive sta-

bility, particularly in the context of guidance forces. By examining how superconducting magnets and coils contribute to the stabilization of the train's lateral position, we seek to gain insights into the forces that prevent the train from deviating off track. This includes analyzing how the dynamic properties of the magnetic fields, such as flux variations, lead to stable motion in the system, thereby ensuring safe and efficient operation. Ultimately, the project aims to contribute to the development of a deeper theoretical understanding of the forces at play, which could aid in the optimization and design of future maglev systems.

## 1.2 EXISTING MAGLEV TECHNOLOGIES - SIMILARITIES AND DIFFERENCES

Two main technologies dominate the maglev train market: Electromagnetic suspension (EMS) and Electrodynamic suspension (EDS). These two technologies both rely on magnetic forces to levitate and accelerate the train, but they entertain very different stabilisation mechanisms to ensure the constant readjustments of the train as it deviates from its normal track. Understanding the difference in the technologies is essential to develop the stabilization processes.

### 1.2.1 • EMS

Electromagnetic suspension (EMS) is one of the two main types of Maglev trains which exist. This system relies on electromagnets on the train, which are attracted to ferromagnetic tracks, lifting the train above the track and eliminating friction.

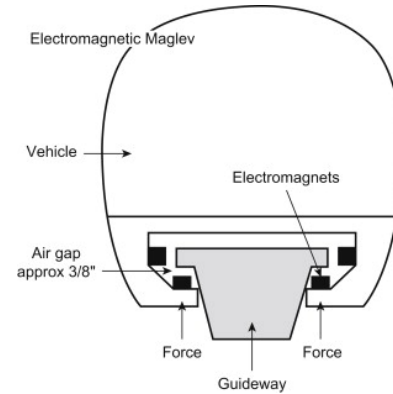


Figure 1: Scheme of the basic functioning of an EMS train

The fundamental mechanism of the EMS system involves the use of active electronic controls to maintain the precise distance between the train and the track. This is achieved by constantly measuring the gap using sensors and adjusting the current in the electromagnets accordingly to stabilize the train's position. The system also incorporates guidance magnets, which ensure that the train stays aligned with the track and does not deviate laterally. Additionally, the active control systems help stabilize the train against pitch, roll, and yaw, as well as other potential instabilities such as sway and surge. This dynamic/active stabilization allows for smooth, high-speed travel with minimal noise and energy loss, making EMS maglev trains an advanced and efficient mode of transportation.

### 1.2.2 • EDS

The basic functioning of an Electrodynamic Suspension (EDS) maglev train relies on the principles of superconductivity and dynamic magnetic interactions between the train and the track. Unlike Electromagnetic Suspension (EMS) trains, which use active magnetic forces to levitate the train, EDS maglev trains utilize the interaction of superconducting magnets on the train with the changing magnetic fields generated by the track to achieve both levitation and guidance. This system is primarily found in Japan (such as the SCMaglev, which is the suspension technology we will study

in depth) and is also being developed for future high-speed rail projects in various countries.

The basic levitation, propulsion and guidance principle of the Japanese EDS train is shown below.

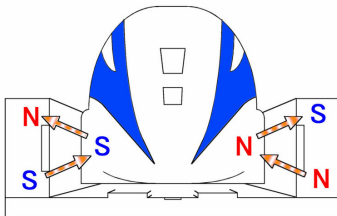


Figure 2: Scheme of the basic functioning of an EDS train (Wikipedia image)

In an EDS system, the train is levitated using superconducting magnets installed on the train, which interact with the coils inside the guideway. The track in an EDS system typically contains a series of coils that create a dynamic magnetic field. When the superconducting magnets on the train move along the track as the train accelerates, the changing magnetic field induces circulating currents in the superconducting magnets, generating repulsive forces that push the train upward, causing it to levitate above the track. This levitation force is passive, meaning it does not require active adjustment or control as in the EMS system. The repulsion between the superconducting magnets and the track keeps the train suspended in a stable position without any physical contact, minimizing friction and allowing for high-speed travel.

It is of interest to us to understand how the EDS system ensure the stability of the interactions between the coils (or superconducting magnets) on the train and on the track. As mentioned, the EDS system relies on passive control and realignment. This means that as the train moves, the magnetic fields generated by the train and the track naturally adjust to maintain the train's stable position. For example, quantitatively, if the train deviates to the left, the magnetic flux from the left side of the train will grow larger than the one on the right. Lens Law tells us that the coils in the left

side of the guideway will induce a force countering this increase in flux, pushing the train back to the right. It is this exact process we wish to modelize in this paper.

## 2

# THEORETICAL BACKGROUND

### 2.1 EMS

Because the magnetic forces alone can lead to an unstable equilibrium, the EMS system relies on active stabilization. This is due to Earnshaw's theorem, citing that a magnetic body cannot remain in equilibrium while being in a magnetostatic field, which is exactly what happens to the ferromagnetic material in the track, subject to the magnetic field created by the train's electromagnets. Therefore there must be some sort of active stabilization to ensure that the height of the train does not vary too much.

The gap between the train and the track is constantly monitored by sensors, and the system adjusts the current flowing through the train's electromagnets to maintain the desired levitation height. If the train begins to drift too far from the track, the system compensates by altering the magnetic field strength, ensuring the train remains suspended at a stable distance. This dynamic adjustment is crucial for the system's stability, as the levitation force changes with variations in the train's speed and position. In summary, anytime the train deviates, an active electronic system readjusts the current flowing through the coils on the train to change the force between the train and the guideway.

The EMS system uses the interaction between the electromagnets located on the train and the guideway to control the lateral displacement. The use of electromagnets implies that the intensity of the magnetic fields are relatively lower compared to the EDS system. However, this also implies that the guidance air gap should be at around 1 cm. There are different types of types of EMS systems. For instance, for the Shanghai Maglev, the

Korean UTM or the Japanese HSST, the levitation and guidance circuits are integrated. The key advantage of this design is that the number of electromagnets is limited to a minimum. However, both systems can interfere, which is a good reason to rather use the other type of EMS system, where the levitation and guidance systems are separated. One example of this is the German Transrapid TR09<sup>1</sup>.

For the sake of simplicity, we make several assumptions in our description of the system. Firstly, we mainly focus on systems where the levitation and guidance systems are disconnected from each other. Secondly, we only consider EMS systems where the force between the guideway and the train is attractive. In such a configuration, the description of the system is the following, as described by Figure 3. The guideway is shaped like an inverted T with two side walls. On one side, the bottom electromagnet, ensuring levitation, is shaped like a U and produces an upward force  $F_{lev}$ , maintaining a vertical airgap  $g_l$ . The side electromagnet, also shaped like a U, provides lateral force to center the vehicle in the guideway. It generates a horizontal force  $F_{gud}$  that maintains a horizontal airgap  $g_g$ . The presence of electromagnets implies magnetic flux paths around each coil. On each side, there are two distinct magnetic circuits: one through the lower levitation electromagnet, one through the upper guidance electromagnet. In all parts concerning the EMS system, we fix the origin at the center of the train. The x-direction is the direction of movement of the train. The y-direction is direction of lateral displacement. Finally, the z-direction is the direction from the bottom of the train to the sky. <sup>2</sup>.

<sup>1</sup><https://link.springer.com/article/10.1007/s40864-019-0104-1>

<sup>2</sup><https://www.emworks.com/en/application/optimizing-magnetic-levitation-for-semi-high-speed-maglev-trains>



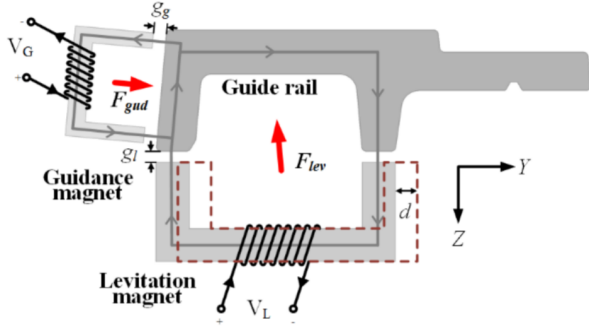


Figure 3: Model of the EMS maglev system

### 2.1.1 • THE MAGNETIC CIRCUIT METHOD

Now let us consider compute the guidance force and the potential energy. There are several methods to compute them. Here we first use consider the two magnetic circuits on each side of the train. We assume the permeability of both electromagnets and the railway to be very high, and the air to have the same permeability as vacuum. Let  $d$  denote the gap between the train and the railway at equilibrium, and  $y$  denote lateral displacement in either direction. Let  $r$  be the radius of the electromagnet. Let us first examine the magnetic circuit on the left side of the train. Let  $I_l$  be the current flowing in the left electromagnet, and  $I_r$  be the current flowing in the right electromagnet. We obtain that the reluctance of the magnetic circuit is given by

$$\mathcal{R}_{total} = \frac{2(d - y)}{\mu_0 \pi r^2}$$

and the magnetomotive force is given by

$$\mathcal{F} = NI_l.$$

Therefore, by Hopkinson's law, we obtain that the magnetic flux circulating in the magnetic circuit is

$$\Phi = \frac{\mathcal{F}}{\mathcal{R}_{total}} = \frac{\mu_0 \pi r^2 NI_l}{2(d - y)}.$$

Thus the magnitude of the magnetic field is

$$B = \frac{\Phi}{\pi r^2} = \frac{\mu_0 NI_l}{2(d - y)}.$$

We obtain that the energy stored in the two air gaps is then

$$U_l = \frac{B^2}{2\mu_0} 2\pi r^2 (d - y) = \frac{\mu_0 N^2 I_l^2 \pi r^2}{4(d - y)}.$$

Moreover, by derivation with respect to the gap  $d - y$ , we obtain the left force:

$$\vec{F}_l(y) = \frac{\mu_0 N^2 I_l^2 \pi r^2}{4(d - y)^2} \vec{e}_y.$$

A more complete derivation can be found in the appendix. Now considering the right side of the train, we obtain similarly that

$$U_r = \frac{\mu_0 N^2 I_r^2 \pi r^2}{4(d + y)}.$$

This yields the right force:

$$\vec{F}_r(y) = -\frac{\mu_0 N^2 I_r^2 \pi r^2}{4(d + y)^2} \vec{e}_y.$$

We deduce the total force on the train:

$$\begin{aligned} \vec{F}_t(y) &= \left( \frac{\mu_0 N^2 I_l^2 \pi r^2}{4(d - y)^2} - \frac{\mu_0 N^2 I_r^2 \pi r^2}{4(d + y)^2} \right) \vec{e}_y \\ &= \frac{\mu_0 N^2 \pi r^2}{4} \left( \frac{I_l^2}{(d - y)^2} - \frac{I_r^2}{(d + y)^2} \right) \vec{e}_y. \end{aligned}$$

### 2.1.2 • THE METHOD OF IMAGES

This is a first approach to approximate the lateral force exerted on the train. Another approach is the method of images. Here, again, let  $d$  denote the gap between the train and the railway at equilibrium, and  $y$  denote lateral displacement in either direction. Let  $L$  be the width of the guideway. We model each electromagnet as two spherical coils of radius  $r$ , one above the other, with opposite current flowing in them. This model is highlighted by Figure 4, where we observe two solenoids around the electromagnet. Here, for simplicity, instead of considering solenoids, we consider two coils of opposite current. The coils are in a plane that is parallel to the face of the guide way facing them. Focusing for instance only one of the left side of the train, we also consider the railway



to be an half space of a high-permeability medium, and the other half space to be vacuum. Recall that the left coil is outside this high-permeability medium, in vacuum. Then, by the image method of point magnetic charges, we get that the potential and fields of the spherical coils were as if the permeable medium was also vacuum but with image magnetic dipoles having the same magnetization. The distance between the magnetic dipole and the boundary between the two half spaces is the same as the distance between the image magnetic dipole and the boundary<sup>3</sup>.

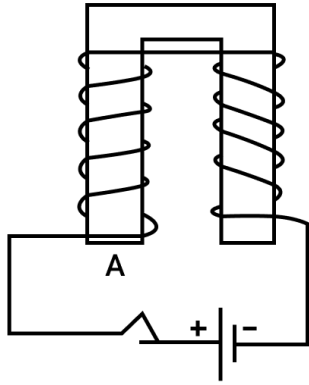


Figure 4: Schematics of an electromagnet

### 2.1.3 • ONE COIL PER ELECTROMAGNET

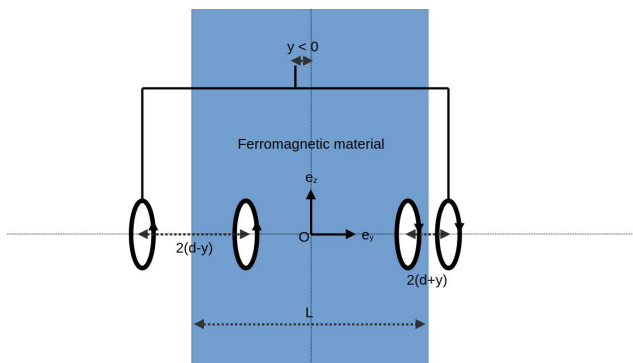


Figure 5: Model of one coil modeling each electromagnet

For simplicity, we will first examine the method of images using one coil per electromagnet instead

of two, and we assume  $r \ll d$  so that we can use the dipole approximation. Each coil on both sides of the train has an image coil that is coaxial and separated by a certain distance as depicted on Figure 5. The image coil is given by reflection with respect to the boundary between the two half spaces. In the appendix, we find that the force exerted by a source coil on a target coil, both of them being coaxial and separated with distance  $y$ , is given by

$$\vec{F} = -\frac{3}{2}\mu_0 II' \pi r^4 \frac{y}{(r^2 + y^2)^{5/2}} \vec{e}_y.$$

Writing

$$f(y) = \frac{3}{2}\mu_0 \pi r^4 \frac{y}{(r^2 + y^2)^{5/2}},$$

we obtain that

$$\vec{F} = -II' f(y) \vec{e}_y.$$

We denote by coil A the coil on the left side of the train, and by coil B the coil on the right side of the train. Now suppose the coil on the left side of the train has current  $I_A$  and the coil on the right side of the train has current  $I_B$ . The force applied on the coil on the left side of the train is then

$$\vec{F}_l(y) = (I_A^2 f(2d-2y) + I_A I_B f(L+2d) + I_A I_B f(L-2y)) \vec{e}_y,$$

and the force applied on the coil on the right side of the train is then

$$\vec{F}_r(y) = -(I_B^2 f(2d+2y) + I_A I_B f(L+2d) + I_A I_B f(L+2y)) \vec{e}_y.$$

The total force applied on the train is then

$$\vec{F}_t = \vec{F}_r + \vec{F}_l.$$

Eventually, the potential energy is given by

$$U_t = - \int \vec{F}_t dy.$$

### 2.1.4 • TWO COILS OF OPPOSITE CURRENT PER ELECTROMAGNET

Here, we examine the method of images using two coils of opposite current per electromagnet, and we

<sup>3</sup>[kirkmcd.princeton.edu/examples/image.pdf](http://kirkmcd.princeton.edu/examples/image.pdf)

don't assume anymore that  $r \ll d$ . As depicted on Figure 6, each real coil as an image coil of the same current. More precisely, the one-coil model using the method of images gave a rough idea of the unstable equilibrium arising in an attractive magnet system. However, this model considered coils as magnetic dipoles, under the assumption that  $d \gg R$ . In the electromagnets in the EMS Maglev guidance system do not feature this characteristic. Moreover, the electromagnet was modeled as the field generated by a single coil, which is a rather limited approximations. Hence, another model was considered. Our second model relies on two aspects:

1. Modeling of the electromagnet: Given the direction of the flux leaving the branches of the electromagnet along the  $y$ -direction, the magnet was modeled as two coils, with same current  $I$  flowing in opposite direction, and located at the end of the branches, i.e. at distance  $l$  from each other and at an air gap  $d \pm x$  from the reaction rail. The coils were superposed  $N/2$  times each, to take into account the  $N$  loops of the solenoid of the electromagnet.
2. Modeling of the force resulting from the behavior of the coils near the ferromagnetic rail: Using the image reflection model with respect to the ferromagnetic plane in the reaction rail, two virtual coils are added asymmetrically. The B-field generated by these were considered to determine the total field on the two real coils (the effect of one real coil to another being considered negligible, as they lie in the same plane and not very far from one another), and finally the Laplace force applied on them. This yields the total force between the reaction rail and the train on one side of the rail.

In this model, the forces from the virtual coils on the real coils are solely taken into account, neglecting the effect of one real coil on the other, on the account that the field in the loop plane and near the loop, is rather weak. In particular, we

use the Laplace force along the  $y$ -axis formula derived in the Appendix (see 4.3), as following:

$$F_y(\rho, y) = -I'R \frac{N^2}{4} \int_{\phi=0}^{2\pi} (B_x \sin \phi + B_z \cos \phi) d\phi.$$

Since the problem is symmetric (for the two real coils), for each side of the rail, one solely needs to compute the force of one real coil and multiply by a factor of 2.

In addition, in the expression of  $F_y$ , of particular importance the the sign of  $I'I$ . If the currents are flowing in the same direction (real coil A - virtual coil A or real coil B - virtual coil B), then  $I'I > 0$ , and if not (real coil B - virtual coil A or real coil A - virtual coil B), we have  $I'I < 0$ .

The total force on one coil can thus be expressed as following, considering a distance  $l$  between the two real coils and a distance  $\Delta y$  as air gap:

$$F = 2(F_y(0, \Delta y) - F_y(l, \Delta y))$$

More precisely, on the left side of the rail,  $\Delta y = 2d - 2y$ , taking as parameter the signed distance  $y$  with respect to equilibrium. This yields

$$F_A(y) = 2(F_y(0, 2d - 2y) - F_y(l, 2d - 2y)).$$

On the right side of the rail  $\Delta y = 2d + 2y$ , but since the geometry is reversed we have

$$\begin{aligned} F_B(y) &= 2(F_y(0, -(2d + 2y)) - F_y(l, -(2d + 2y))) \\ &= 2(F_y(l, 2d + 2y) - F_y(0, 2d + 2y)). \end{aligned}$$

The total force on the train can then be expressed as the sum of these two signed forces:

$$F_{tot}(y) = F_A(y) + F_B(y).$$

Finally, this yields the potential energy  $U_y$ , by the formula:

$$F_{tot}(y) = -\frac{dU_y}{dy}.$$

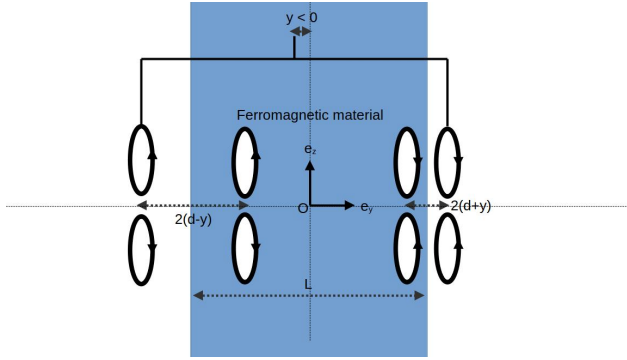


Figure 6: Model of two coils modeling each electromagnet

## 2.2 EDS

We now detail the derivation of the potential energy in function of lateral displacement of the train. Our goal is to show there exists a potential well, and that the system is self-sufficient in bringing the train back to its equilibrium position. We will firstly detail our simplified train model, which is satisfactory in proving the magnetic dipole properties of the Maglev EDS train. Then we derive the flux on the guideway coils created by the train coils, allowing us to determine an induced magnetic field and the magnetic potential energy.

### 2.2.1 • MODEL

Our train model is a simplified one of the real functioning of the SCMaglev train. This section is dedicated to understanding our model, the variables and degrees of freedom of the system.

The scheme below gives an overview of our train model, and we justify later why this is satisfactory.

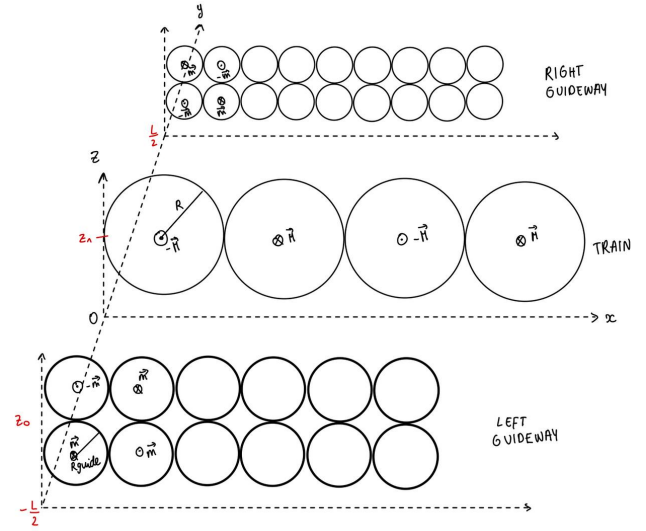


Figure 7: Scheme of our model for the SCMaglev train

In this model the main points are as follows:

- The train is assumed to have no width: this is a simplification we have chosen to make because a regular EDS train is made of superconducting coils on each side of the train, where both sides of the train have opposing poles (ie: if there is a north pole on the right, the same coil on the left will be a south). Hence the train can be seen as one big dipole, which makes our computations simpler later on, and allows us to look at the lateral displacement of this dipole.
- The coils on the train are superconducting, and their magnetic dipole moment alternates in sign.
- We suppose the train to be 4 coils long, this is an assumption we can make without loss of generality, as the 5th coil showed to have little impact on the flux on a single guideway coil.
- The guideway is made of 8-shape coils, which can be separated into 2 circle coils one on top of the other, having opposite moment sign.

We can now precisely describe the variables and coordinates of our system.

### Global coordinate system

- $x$ : direction of motion of the train.
- $y$ : lateral (horizontal) direction;  $y = 0$  when train is centered.
- $z$ : vertical (levitation) direction.

### Train Coils

- Radius:  $R$
- Indexed by  $h \in \{1, 2, 3, 4\}$
- Coil center positions:
  - $x_h = vt + (2h - 1)R$
  - $y$  (lateral displacement)
  - $z = z_1$
- Magnetic dipole moment:  $\mathbf{M}_h = (-1)^h I \pi R^2 \mathbf{e}_y$
- $I$  is supposed to be constant

### Guideway Coils

- Radius:  $R_{\text{guide}}$
- 2 figure-8 coils per side (left and right), indexed by  $j \in \{1, 2\}$
- Coil center positions:
  - $x_j = (2j - 1)R_{\text{guide}}$
  - $y_j = \mp \frac{L}{2}$  (minus for left side, plus for right side)
  - $z = z_0 \pm R_{\text{guide}}$  (top and bottom loops respectively)

### Relative Position Vector

The vector from train coil  $h$  to guide loop ( $j$ , side, loop) is:

$$\mathbf{R}_{h,j}^{\text{side,loop}} = \begin{pmatrix} x_j - x_h \\ \pm \frac{L}{2} - y \\ z_0 \pm R_{\text{guide}} - z_1 \end{pmatrix}$$

For example, the position vector from the center of the 1st train coil to the center of the top right first guideway coil is:

$$\mathbf{R}_{1,1}^{\text{right,top}} = \begin{pmatrix} R_{\text{guide}} - R - vt \\ \frac{L}{2} - y \\ z_0 + R_{\text{guide}} - z_1 \end{pmatrix}$$

For simplification during our computations, we will write this vector  $\mathbf{r}$ .

Final coordinates With the following parameters: For most of our computations, and to simplify notations, we use the following coordinates:

$$x_h = vt + 2(h - 1)R$$

$$X = x - x_h$$

$$Y = \pm \frac{L}{2} - y$$

$$Z = z_0 - z_1 \pm R_g$$

$$r^2 = X^2 + Y^2 + Z^2$$

### 2.2.2 • APPROACH

Our ultimate goal is to understand the behavior of the potential energy in function of the lateral position of the train. To achieve this, we begin by assuming a constant current through the coils of the train. This creates a changing magnetic field, as the train moves at constant velocity  $v$ .

This changing magnetic field induces a current in the guideway coils. In order to obtain this current, we compute the magnetic flux of the 4 train coils over each guideway coil. Once this current is derived, and since we can approximate the guideway coils as alternating magnetic dipoles, we can compute the induced B-field. After deriving each of these formulas, our goal is to simulate the real behavior of the system as closely as possible by summing the induced B-fields of each guideway coil, and ultimately summing the potential energy profiles of each of the train coils. All of this is done in a Python simulation, using our detailed computations below. The details of all the derivations and computations are in the appendix of this paper.

### 2.2.3 • COMPUTATION OF THE FLUX AND INDUCED CURRENT

The motion of the train induces a current on each of the guideway coils that results in the guidance magnetic field. We first establish the magnetic flux by the train's magnetic field through each guide coil of the train. The exact derivations of

the flux and current are in the appendix.

In order to compute the flux through each guideway coil, we must compute the B-field emitted by each train coil, which depends on the magnetic dipole moment of the superconducting coil.

In this model, we make an **important assumption**, which is that the radius of the guideway coils is small enough so that the B-field emitted by the train coil is **uniform** all over the guideway coil. Therefore, the B-field at any point on the guideway coil is the same as the one at the center of the guideway coil.

$$\mathbf{B}(\mathbf{R}) = \mathbf{B}(\mathbf{R}_{h,j}^{\text{side,loop}})$$

where  $\mathbf{R}$  is the position vector between the center of the  $h$  train coil and an arbitrary point on the guideway coil. To simplify, we write  $\mathbf{R}_{h,j}^{\text{side,loop}} = \mathbf{r}$  in the next computations.

The formula for the B-field emitted by one train coil is:

$$\mathbf{B}(\mathbf{r}) = \frac{\mu_0}{4\pi} \frac{3(\mathbf{M}_h \cdot \mathbf{r})\mathbf{r} - \mathbf{M}_h r^2}{r^5}$$

And the total B-field at the center of guideway coil  $j$  (top/bottom and left/right) from the train (4 coils) writes:

$$\mathbf{B}_{\text{tot},j}^{\text{side,loop}} = \sum_{h=1}^4 \frac{\mu_0}{4\pi} \frac{3(\mathbf{M}_h \cdot \mathbf{r})\mathbf{r} - \mathbf{M}_h r^2}{r^5}$$

For each guideway coil, the train's magnetic field induces a flux. We are interested in computing the magnetic flux of the B-field emitted by one train coil over one 8-shape guideway coil. Since these guideway coils are 8-shape, the current in the loop should be the same. This is why we compute the flux over one whole 8-shape coil.

By our assumption of uniformity of the B-field over one whole guideway coil, the final formula for  $\Phi$  is:

$$\Phi = \int_S \mathbf{B} \cdot d\mathbf{S} = \mathbf{B}(\mathbf{r})\pi R_{\text{guide}}^2$$

This is due to the uniformity of the B-field over one guideway coil: the flux ends up simply being the multiplication of our uniform B-field by the surface we are considering. This assumption simplifies our computations greatly, allowing us to focus on the next derivations. After simplifications and developing this formula, we get that:

$$\Phi_{h,j}^{\text{side,loop}} = \frac{\mu_0 M_h R_{\text{guide}}^2}{4} \cdot \frac{3Y^2 - r^2}{r^5}$$

Now, considering the contribution of every train coil, the total flux over one 8-shape guideway coil reads:

$$\begin{aligned} \Phi_j^{\text{side}} &= \sum_{h=1}^4 \Phi_{h,j}^{\text{side,top}} - \Phi_{h,j}^{\text{side,bottom}} \\ &= \sum_{h=1}^4 \frac{\mu_0 M_h R_{\text{guide}}^2}{4} \left[ \frac{3Y^2 - r_+^2}{r_+^5} - \frac{3Y^2 - r_-^2}{r_-^5} \right] \end{aligned}$$

with

$$r_{\pm}^2 = X^2 + Y^2 + (z_0 \pm R_{\text{guide}} - z_1)^2$$

We now use Lens' Law and Ohm's Law to derive the induced current. We firstly compute the electromagnetic force  $\epsilon$ :

$$\begin{aligned} \epsilon &= -\frac{d\Phi}{dt} \\ &= \sum_{h=1}^4 \frac{v\mu_0 M_h R_{\text{guide}}^2}{4} \left[ \left( \frac{-2X}{r_+^5} + \frac{5X(3Y^2 - r_+^2)}{r_+^7} \right) \right. \\ &\quad \left. - \left( \frac{-2X}{r_-^5} + \frac{5X(3Y^2 - r_-^2)}{r_-^7} \right) \right] \end{aligned}$$

Ohm's law then gives the current of one specific 8-shape guideway coil, by dividing by the resistance:

$$i_j^{\text{side}} = \frac{\epsilon}{R_e}$$

where  $R_e$  is the resistance of the guideway coils. When running a numerical simulation of the evolution of the current going through a fixed guideway coil in function of time, we find that the current is oscillatory, and has a specific period and frequency. It is by time-averaging over this period of

current that we will be able to find the potential energy in function of the lateral position.

Having derived this current allows us to deduce the induced B-field emitted by the guideway of the SCMaglev train. This induction process is exactly the way the train stabilizes.

#### 2.2.4 • INDUCED B-FIELD AND FINAL EXPRESSION OF U

As for the train coils, the guideway dipoles generate a dipole moment which we will name  $\mathbf{m}_j^{\text{side,loop}}$ . Similarly as for the train, the current in the guideway coils alternates in sign between the top and bottom, between the left and right. This alternation in signs of the dipoles is what allows for the train to levitate and be propelled forward. The train coils are subject to alternating magnetic fields, and therefore are attracted and pushed away by the guideway periodically. This allows the train to move forward. We can write:

$$\begin{aligned}\mathbf{m}_j^{\text{side,top}}(t) &= +i_j^{\text{side}}(t) \cdot \pi R_{\text{guide}}^2 \cdot \mathbf{e}_y \\ \mathbf{m}_j^{\text{side,bottom}}(t) &= -i_j^{\text{side}}(t) \cdot \pi R_{\text{guide}}^2 \cdot \mathbf{e}_y\end{aligned}$$

We then remind the formula for the B-field generated by a loop of current  $i$ , with dipole moment  $\mathbf{m}$ :

$$\mathbf{B}(\mathbf{r}) = \frac{\mu_0}{4\pi r^5} \left[ 3(\mathbf{m} \cdot \mathbf{r})\mathbf{r} - r^2 \mathbf{m} \right]$$

We would like to express the potential energy felt by one single train coil from the 4 8-shape guideway coils we consider: recall they are labeled by  $j \in \{1, 2\}$ , top/bottom, left/right. To do this, we must express the B-field emitted by the top and bottom dipole for each 8-shape coil at the center of train coil  $p$ . We recall the formula for the magnetic potential energy of a magnetic dipole in an external magnetic field is:

$$U = -\mathbf{M} \cdot \mathbf{B}$$

Now, since the dipole moments of the train coils are in the  $\mathbf{e}_y$  direction, we will only compute the

y-component of the B-fields. We have that:

$$\begin{aligned}B_{j,p}^{\text{side}}(t)_y &= B_{j,p}^{\text{side,top}}(t)_y + B_{j,p}^{\text{side,bottom}}(t)_y \\ &= \frac{\mu_0 m_j^{\text{side,top}}(t)}{4\pi(r_{\text{top}}^2)^{5/2}} \left[ 3Y'^2 - r_{\text{top}}^2 \right] \\ &\quad + \frac{\mu_0 m_j^{\text{side,bottom}}(t)}{4\pi(r_{\text{bottom}}^2)^{5/2}} \left[ 3Y'^2 - r_{\text{bottom}}^2 \right]\end{aligned}$$

(see appendix for detail of the coordinates and computations). Now having the each B-field on each train coil, we simply have to sum over all guideway coils and all train coils to obtain the total potential energy. We firstly express the potential energy of one train coil:

$$\begin{aligned}U(t, y)_p &= -M_p \sum_{\text{side} \in \{\text{left}, \text{right}\}} \sum_{j=1}^2 \left( \right. \\ &\quad B_{j,p}^{\text{side,top}}(t, y)_y + \\ &\quad \left. B_{j,p}^{\text{side,bottom}}(t, y)_y \right)\end{aligned}$$

We can then sum over  $p$  to get the potential energy of the whole train.

$$\begin{aligned}U(t, y) &= -\sum_{p=1}^4 M_p \sum_{\text{side} \in \{\text{left}, \text{right}\}} \sum_{j=1}^2 \left( \right. \\ &\quad B_{j,p}^{\text{side,top}}(t, y)_y + \\ &\quad \left. B_{j,p}^{\text{side,bottom}}(t, y)_y \right)\end{aligned}$$

To compute the total magnetic potential energy  $U(t, y)$  of the train, we account for every interaction between each train coil and the magnetic field generated by the induced magnetic dipole moments in the guideway coils.

- The train is composed of 4 superconducting coils, indexed by  $p \in \{1, 2, 3, 4\}$ , each carrying a fixed dipole moment  $\mathbf{M}_p$  and located at a distinct  $x$ -position, but sharing the same lateral displacement  $y$ .
- The guideway consists of two sides (left and right), and on each side, there are 2 guideway coils indexed by  $j \in \{1, 2\}$ .



- Each guideway coil is a figure-8 coil, made of a top loop and a bottom loop, each modeled as a separate magnetic dipole moment.
- For each pair guideway coil:
  - We compute the induced current in the guideway coil due to the magnetic flux from all 4 train coils.
  - Use this current to compute the dipole moment of the top and bottom loops,
  - Compute the magnetic field produced by each loop at the position of train coil  $p$ ,
  - And evaluate the interaction energy as  $-\mathbf{M}_p \cdot \mathbf{B}$ .

This results in a double sum over:

- The 4 train coils ( $p$ ).
- The 2 guideway coils per side ( $j \in \{1, 2\}$ ).
- The 2 sides (left and right).
- And within each guideway coil, the top and bottom loops.

Thus, for each train coil  $p$ , we compute the contribution from 4 guideway positions (2 sides  $\times$  2 positions), and for each, we evaluate both top and bottom loops, leading to 8 contributions per train coil. In total, the energy sum includes 32 interaction terms.

This formula accounts for all contributions to the magnetic potential energy of the train at time  $t$  and horizontal position  $y$ . It will form the basis of the stability analysis by evaluating the curvature of  $U(y)$ .

### 3

## NUMERICAL SIMULATIONS

### 3.1 EMS

#### 3.1.1 • THE MAGNETIC CIRCUIT METHOD

Depending on the method to derive the lateral force and the potential energy, more or less work was required in this part of the project. Considering the magnetic circuit method, the potential obtained is

$$U_t = \frac{\mu_0 N^2 I_r^2 \pi r^2}{4(d-y)} + \frac{\mu_0 N^2 I_l^2 \pi r^2}{4(d+y)},$$

and the force obtained is

$$\vec{F}_t = \frac{\mu_0 N^2 I_l^2 \pi r^2}{4(d+y)^2} \vec{e}_y - \frac{\mu_0 N^2 I_r^2 \pi r^2}{4(d-y)^2} \vec{e}_y.$$

We plot the corresponding equations by choosing relevant data inputs<sup>4</sup>:

1. Number of coils  $N = 210$ ;
2. Current in the right electromagnet  $I_r = 57$  A;
3. Radius of the coils  $r = 6$  cm;
4. Gap between the train and the railway  $d = 11$  mm.

We also take the current ratio given by  $I_r/I_l$  as parameter where  $I_l$  is the current in the left electromagnet, and we vary this current ratio to plot several curves, given in the next section. The code is in the Appendix.

#### 3.1.2 • THE METHOD OF IMAGES: ONE COIL PER ELECTROMAGNET

Considering the image method applied to an electromagnet modeled by one single coil, we obtain

<sup>4</sup><https://koreascience.kr/article/JAKO201709641401416.pdf>



in the previous section that the force exerted on the train as a function of the lateral displacement  $y$  is given by:

$$\vec{F}_t(y) = (I_A^2 f(2d - 2y) - I_B^2 f(2d + 2y))$$

$+ I_A I_B f(L - 2y) - I_A I_B f(L + 2y)) \vec{e}_y$ , where

$$f(y) = \frac{3}{2} \mu_0 \pi r^4 \frac{y}{(r^2 + y^2)^{5/2}}.$$

Eventually, the potential energy is given by

$$U_t = - \int \vec{F}_t dy.$$

We plot the corresponding equations by choosing relevant data inputs<sup>5</sup>:

1. Current circulating in coil A  $I_A = 57$  A;
2. Radius of the coils  $r = 2$  mm;
3. Gap between the train and the railway  $d = 11$  mm.
4. Width of the guideway  $L = 4.0$  m

Here, for the radius of coils, we don't take  $r = 6$  cm as it is in reality but we take  $r = 2$  mm so that the condition for the dipole approximation is still valid:  $r \ll d$ . This will be taken into account in the next section as it has an effect on the magnitude of the force obtained. We also take the current ratio given by  $I_B/I_A$  as parameter, where  $I_B$  is the current in the coil B and we vary this current ratio to plot several curves, given in the next section. The code is in the Appendix.

### 3.1.3 • THE METHOD OF IMAGES: TWO COILS OF OPPOSITE CURRENT PER ELECTROMAGNET

Here, the use of numerical tool is much more extensive than before as the elliptic integrals are computed numerically for the determination of the magnetic field at a specific points. Moreover, instead of using a dipole approximation, we integrate numerically the infinitesimal Laplace force

to compute the total force on the entire target loop. This allows us to keep accurate data constants. The computation of  $U$  and the making of graphs remains however the same as previously.

We plot the corresponding equations by choosing relevant data inputs<sup>6</sup>:

1. Number of superposed coils  $N = 210$ ;
2. Current circulating in coil A above  $I = 57$  A;
3. Radius of the coils  $r = 6$  cm;
4. Gap between the train and the railway  $d = 11$  mm.
5. Width of the guideway  $L = 4.0$  m

The code is in the Appendix.

## 3.2 EDS

Our ScMaglev train models calls for developed and difficult computations depending on many parameters which vary in time and in space. These physical quantities are difficult to picture without the use of numerical simulations. Our analytical computations can only take us so far, and quantities such as the current in the coils call for simulating their behavior to determine if they are periodic or not, and if they are what is the period of oscillation.

Our other goal in using a numerical simulation is to clearly plot the potential energy profile in function of the lateral displacement of the train. This plot is at the heart of this project, as it will allow us to come to a conclusion as to the stability of the Maglev train when it is displaced from its equilibrium position at the center of the rail.

One of our challenges in these simulations was choosing parameters that allowed us to get the best idea of the real behavior of the train. We debated summing the energy over more than 4

<sup>5</sup><https://koreascience.kr/article/JAKO201709641401416.pdf> <sup>6</sup><https://koreascience.kr/article/JAKO201709641401416.pdf>

train coils, or summing the B-fields of a very large amount of guideway coils instead of just 2 8-shape coils on each side. However, as explained in the end of the theory section, we resorted to restricting the train to 4 coils and the guideway to 4 8-shape coils: 2 on each side. We realized that this simplification was sufficient to understand the behavior of the train after simulating over more coils. We therefore compute 16 induced magnetic fields in our simulations, which then allow us to plot the potential energy over one train coil, which is the sum of the potential energies from each guideway coil.

### 3.2.1 • PARAMETERS

As mentioned previously, we modelize our train as 4 train coils and 4 8-shape loop coils. It is essential to choose parameters which modelize reality correctly.

Parameter	Symbol	Value
Current passing in the train's coils	$I$	$7 \times 10^5 A$
Resistance in the guide-way coils	$R_E$	$10\Omega$
Velocity of the train	$v$	$v_{slow}, v_{fast}$
Height of the Train	$z_1$	$0.7m$
Height of the guideway coil	$z_0$	$:= 0m$
Distance between the train and the guide-way	$L$	$1.2m$
Radius of the guide-way coils	$R_{guide}$	$1m$
Radius of the train's coils	$R_{train}$	$1.5m$

Table 1: Parameters used in the simulation

Throughout our simulation, our goal is also to explore different velocity regimes of the train, therefore we decided to plot the current for  $v_{slow} = 30 m.s^{-1}$  (slower regime) and  $v_{fast} = 160 m.s^{-1}$  (about the max velocity of the train)

### 3.2.2 • PROCEDURE

The simulation works in two parts: First to establish the Magnetic field through the guideway system induced by the train, then it computes the energy observed by the train during its traversal through this specific induced magnetic B-field, which we average with regards to time.

In order to achieve the guide way coil's current and to observe the periodic signal induced by the train's geometry and its motion, we model the studied guide way to be slightly further than the origin, at  $x_{coil} = 90m$  so that the train takes some time to travel to it, allowing a proper study of the induced current. This induced current on the guide coil consists of derivative of the sum of the flux on each loop of the eight-coil. When computing the magnetic field induced by one such eight-coil, we impose that

$$I_{j,p}^{side,top} = -I_{j,p}^{side,bottom}$$

Each guide way coil dipole is computed this way and allows us to compute precisely the Magnetic field through one eight-coil slice.

The B-field is restricted to be only along the y-axis due to the orientation of the train's magnetic dipole. Since the current is periodic through a traversal of the train, we will compute the average potential energy the train is submitted to over one period of its traversal, which indicated the effective field the train is subjected to. We want to study how the lateral position of the train affects the magnetic field it is subjected to, so we study over the possible train positions along the y-axis, and its effect to the average potential, while we the  $z$  and  $x$  position of the train to be relevant to the coordinates of the guide coils.

## 4

# RESULTS AND DISCUSSION

### 4.1 EMS

#### 4.1.1 • THE MAGNETIC CIRCUIT METHOD

From the simulation, we obtain the lateral forces and the corresponding potential energy as a function of lateral displacement. Firstly, we consider the case where  $I_A = -I_B = 57\text{ A}$  and obtain Figure 8. We observe that the equilibrium is unstable, which means that a little displacement in the  $y$  direction will lead to a force encouraging further displacement in the  $y$  direction. Moreover, we observe that the amplitude of the force is very high. This can be due to several reasons, the main being probably magnetic flux leakage. Indeed, we assumed that the magnetic flux stay confined within the circuit. However, some flux escapes the intended path. The leakage increases with the size of the air gap, hence this causes the amplitude of the force to be overestimated. We now consider the case where  $I_A = 57\text{ A}$  and  $I_B = -5.7\text{ A}$ , and obtain Figure 9. We observe that for little displacement  $y < 0$ , the force remains positive, which means the train is encouraged to come back to its original position. This highlights how the guidance system may work. Indeed, the unstable equilibrium implies the need for position sensors that the vertical gap between the train and guideway and lateral side position. The system adjusts the current in the electromagnets thousands of times per second to maintain stable levitation, correct alignment in curves and turns and compensation for external forces like wind, weight shift, or track imperfections. In particular, our model shows that if we decrease the current to a factor of  $1/10$  for one of the two electromagnet, we get that the train is encouraged to come back to its original position.

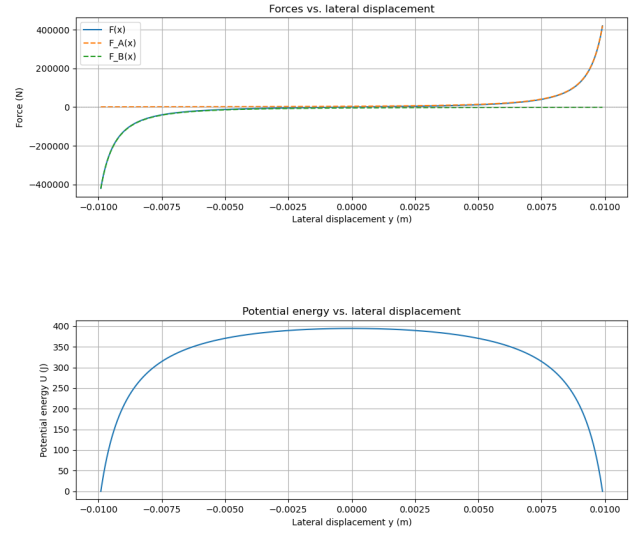


Figure 8: Lateral forces and corresponding potential energy as a function of lateral displacement when  $I_A = -I_B = 57\text{ A}$  using the magnetic circuit method.

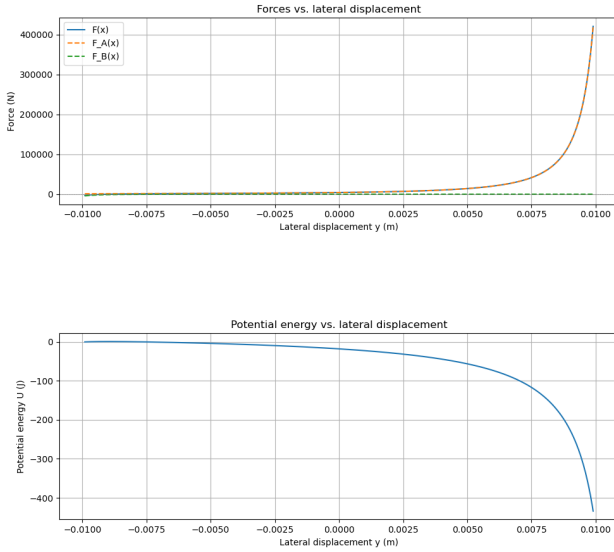


Figure 9: Lateral forces and corresponding potential energy as a function of lateral displacement when  $I_A = 57$  A and  $I_B = -5.7$  A using the magnetic circuit method

#### 4.1.2 • THE METHOD OF IMAGES: ONE COIL PER ELECTROMAGNET

From the simulation, we obtain the lateral forces and the corresponding potential energy as a function of lateral displacement. Firstly, we consider the case where  $I_A = -I_B = 57$  A and obtain Figure 10. In particular, we observe that the equilibrium is unstable, which means that a little displacement in the  $y$  direction will lead to a force encouraging further displacement in the  $y$  direction. Furthermore, we observe that the amplitude of the force is very low. This is due to the fact that we only used a single coil, and the intensity of the magnetic field it generates is very far from the intensity of the magnetic field of an electromagnet of the same radius. Similarly as before, we now consider the case where  $I_A = 57$  A and  $I_B = -5.7$  A, and obtain Figure 11. We observe that for little displacement  $y < 0$ , the force remains positive, which means the train is encouraged to come back to its original position.

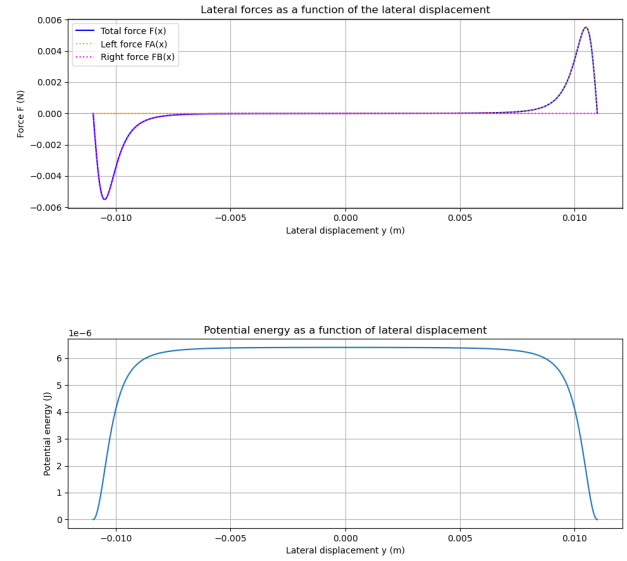


Figure 10: Lateral forces and corresponding potential energy as a function of lateral displacement when the  $I_A = -I_B = 57$  A using the method of images for one coil as a model of an electromagnet

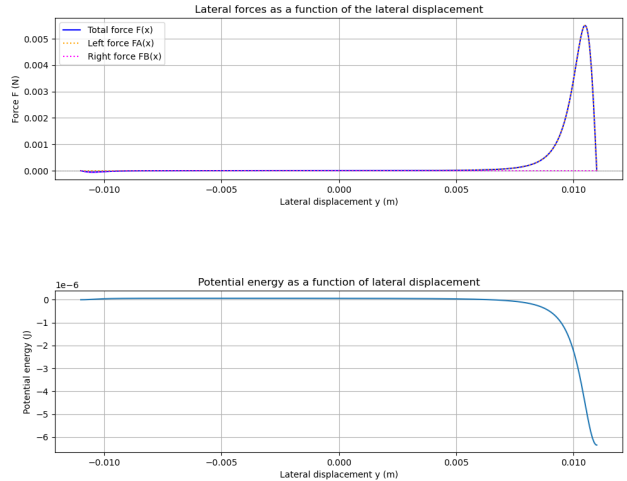


Figure 11: Lateral forces and corresponding potential energy as a function of lateral displacement when the  $I_A = 57$  A and  $I_B = -5.7$  A using the method of images for one coil as a model of an electromagnet

#### 4.1.3 • THE METHOD OF IMAGES: TWO COILS OF OPPOSITE CURRENT PER ELECTROMAGNET

From the simulation, we obtain the lateral forces and the corresponding potential energy as a function of lateral displacement. We consider the case where  $I = 57\text{A}$  and obtain Figure 12. We observe that the equilibrium is unstable, which means that a little displacement in the  $y$  direction will lead to a force encouraging further displacement in the  $y$  direction. We observe that the amplitude of the force is relatively the same as the one in reality. This is the best model we obtained. One key element of this model is that the rate of increase of the amplitude of the force decreases eventually with the lateral displacement. This matches completely the reality, being close to curves obtained experimentally<sup>7</sup>. Similarly as before, we now consider the case where  $I_A = 57\text{ A}$  and  $I_B = -5.7\text{ A}$ , and obtain Figure 13. We observe that for little displacement  $y < 0$ , the force remains positive, which means the train is encouraged to come back to its original position.

<sup>7</sup>[dspace.mit.edu/handle/1721.1/16351](https://dspace.mit.edu/handle/1721.1/16351)

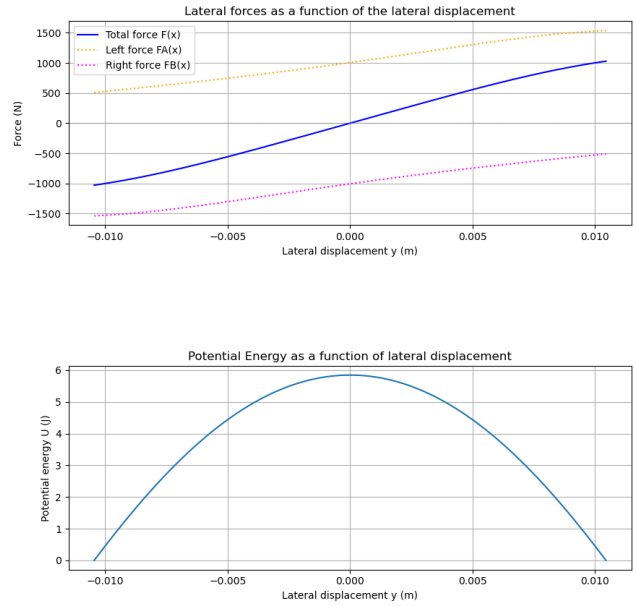


Figure 12: Lateral forces and corresponding potential energy as a function of lateral displacement when the  $I_A = -I_B = 57\text{ A}$  using the method of images for two coils as a model of an electromagnet

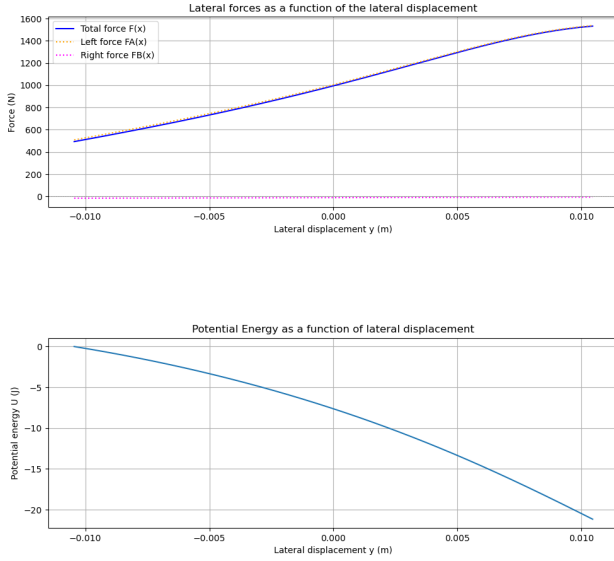


Figure 13: Lateral forces and corresponding potential energy as a function of lateral displacement when the  $I_A = 57$  A and  $I_B = -5.7$  A using the method of images for two coils as a model of an electromagnet

#### 4.1.4 • SUMMARY AND FURTHER IMPROVEMENTS

The different models used to study the guidance force allowed us to consider the problem with different angles. The magnetic circuit model allows to study how magnetic fluxes and forces develop in the system {electromagnet + ferromagnetic rail}. By representing the magnetic path using reluctance and magnetomotive forces, it simplifies the complex 3D field interactions into a tractable form. Transitioning to the two-coil model introduces another view, using mirror image assumption to compute actual forces between the electromagnet, modelled as coils, with the ferromagnetic surface. In addition, the two models capture the unstable equilibrium arising, by which any lateral displacement from the central position increases the magnetic pull from the nearer pole, reinforcing the deviation rather than correcting it. This highlights the need for active stabilization, but with the ad-

vantage of avoiding oscillatory regimes in a stable equilibrium.

However, both models come with important limitations. The magnetic circuit model, by its nature, ignores fringing fields, as well as the non-linearity of the ferromagnetic material, and the actual spatial distribution of magnetic fields. It assumes uniform cross-sections and linear permeability, which do not reflect real materials or geometries. On the other hand, the two-coil model still relies on significant simplifications, especially in the assumption that the mirror image approximation model fits perfectly (the surface of the ferromagnetic surface is not in its essence a simple plane). Despite these limitations, both models successfully highlight the core challenge of EMS guidance: maintaining stability around an inherently unstable equilibrium point. They also demonstrate that by carefully modulating the currents in the guidance coils, lateral control is achievable, and the system can be steered without any mechanical contact. As a next step, model accuracy could be improved by incorporating nonlinear magnetic properties. An improved model could include inhomogeneity, saturation, and the influence of detailed rail geometry. Finally, while we considered the structure with separated guidance and levitation electromagnets, it could be interesting to dig into the other system, where levitation and guidance are controlled using a single pair of electromagnets. This could allow for an efficiency comparison.

Concerning the simulations with Python, they have proven to be accurate and reliable within the assumptions of both models. Using numerical and elliptic integration has also proven to be precise, enabling us to have consistent and accurate results, as well as reducing the computational complexity of direct integral computations. The curves obtained have a shape comparable to actual practical guidance curves found in articles studied (see References for more detail), giving more assurance to our models.



## 4.2 EDS

### 4.2.1 • GUIDEWAY COIL CURRENT

Our first objective in the numerical simulation of our model is to obtain the plot of the induced guideway coil current with respect to time  $i(t)$ . Plotting this current has several objectives for us:

- Plotting the current allows us to verify that we do obtain a periodic oscillatory current, as expected. We can therefore make sure that our assumptions when computing the flux and current were not unrealistic, and that they do not differ from the reality of the current.
- By numerically simulating the current, we can obtain important information such as its oscillation frequency, period and amplitude. These values are necessary for us to get an accurate potential energy profile, as we will time-average the potential energy of a coil over one current oscillation period.

We obtained the following plot for the current through one guideway 8-coil loop, as the current is constant throughout the whole loop, as shown in Figures 14 and 15.

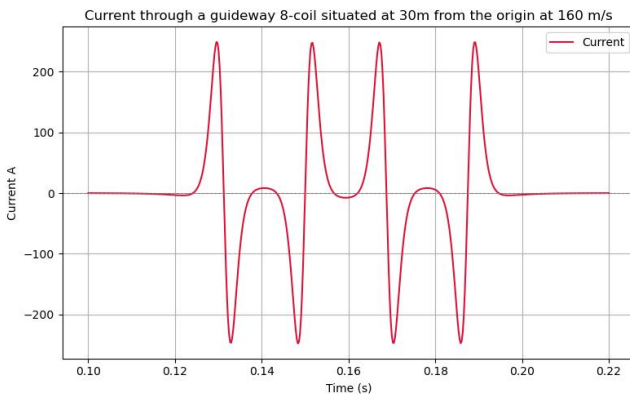


Figure 14: Induced current simulation for an 8-shape coil with  $v = 160 \text{ m.s}^{-1}$

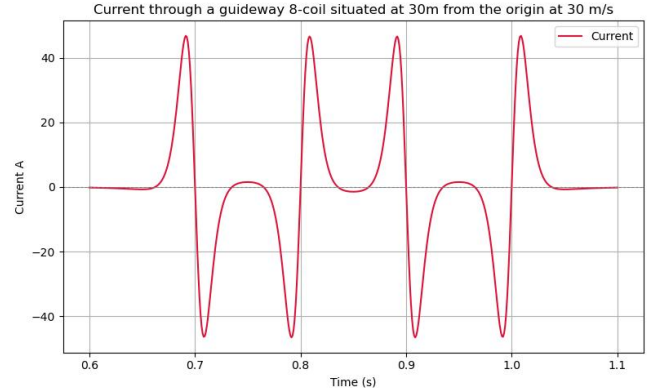


Figure 15: Induced current simulation for an 8-shape coil with  $v = 30 \text{ m.s}^{-1}$

Due to the arrangement of the train coils in a sequence of alternating magnetic dipoles, the induced current follows a periodic pattern as the train traverses through it. The period and frequency of this oscillating current is then computed using a fast Fourier transform, and the period will allow us to find the time average of the energy felt by the train during its traversal through the myriad guide coils.

$v \text{ (m} \cdot \text{s}^{-1}\text{)}$	Max frequency (Hz)	Period (ms)
160	68.50	15
30	14.97	67

Table 2: Results from the FFT of the two signals

### 4.2.2 • POTENTIAL ENERGY

Finally, we simulate the B-field emitted by all guideway coils (32 fluxes and fields), which allow us to arrive at a profile for the potential energy of the system.

We would like to obtain a potential energy plot which justifies that when the train deviates to the left or right, the process of induction and the increasing flux on one guideway creates a restoring force that pushes the line of dipoles back to its equilibrium point.



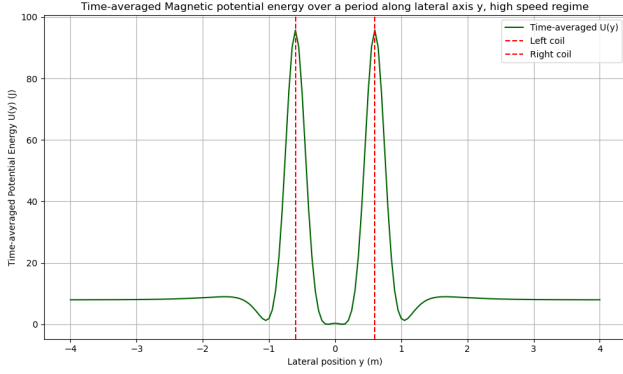


Figure 16: Potential Energy profile for the high-speed arrangement

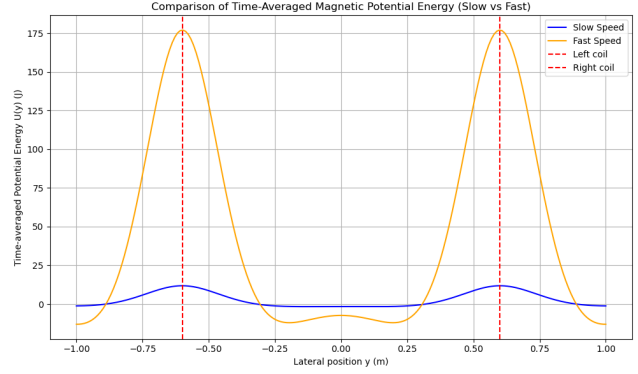


Figure 18: Potential Energy profile for the low-speed arrangement

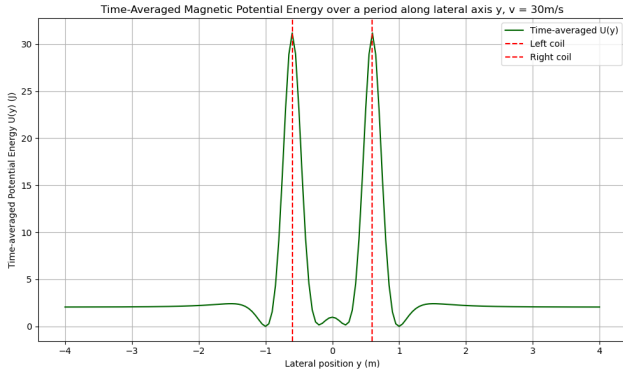


Figure 17: Potential Energy profile for the low-speed arrangement

The two graphs exhibit a "potential well" structure with the borders the two guide way tracks' positions. Both of them admit two absolute minima, with a "bump" at the center of the space. There are two noticeable differences between the two graphs: their magnitudes and the accentuated presence of a bump in the center for the slow configuration. Although more accentuated, the central bump of the slow configuration has a smaller norm than that of the fast configuration.

To overcome the potential barrier, the train must receive a horizontal kinetic energy that is superior to 100 Joules for the high, cruising velocity configuration, while for the slower velocities, 30 Joules will be sufficient. Moreover, due to the more accentuated central bump, small perturbations is also likely to cause more turbulence during the train's function. Hence, it is necessary for the train to run at a very high velocity, which is chosen as the velocity required for levitation and used for cruising, for the train to have a robust lateral stability.

Using Python-based numerical simulations, we computed the induced current as a function of type and plotted the potential energy profile at both high and low speeds. It verified the passive stable levitation at sufficient speeds. In fact, our results confirmed that EDS naturally stabilizes the train laterally due to its dependence on motion-induced currents and repulsive magnetic forces, distinguishing it from the inherently unstable EMS configuration.

## 5

# CONCLUSION

---

In conclusion, this study of the guidance of EMS and EDS Maglev train allowed to have an idea of how to sustain stability of such systems, which clearly stand out from previous train technologies. Both EMS and EDS systems were successfully modeled and analyzed thanks to simplified physical models with accurate numerical implementation using Python.

As illustrated by our models, while the EMS Maglev guidance relies on an unstable equilibrium, by modifying the current of guidance electromagnets, one can successfully control the equilibrium position. The EDS, on the other hand, employs repulsive mechanism which leads to a stable equilibrium, as captured by our model. Today, EMS Maglev trains are a commercially deployed technology (primarily used in Japan, South Korea, and China). One most well-known example is the Shanghai Maglev Train, in operation since 2004 and uses the Transrapid technology. It achieve speeds up to 430 km/h.

Looking to the future, EMS maglev trains are expected to become more widespread as countries invest in cleaner, faster, and more efficient transportation. The potential for speeds above conventional rail, coupled with lower maintenance due to the absence of mechanical contact, makes EMS systems especially attractive. EMS faces competition from the EDS systems, which provide a stable equilibrium at high speeds without active feedback. While EDS allows for higher top speeds and greater energy efficiency at cruise, it typically requires complex cryogenic systems and higher minimum operating speeds to generate lift, which can limit its flexibility for frequent stops or lower-speed travel. Thus EMS systems could take profit of their simpler infrastructure and be used extensively in urban or medium-speed contexts due to their low-speed operability. One should never-

theless not neglect their need for continuous active control introduces higher system complexity in terms of electronics and safety mechanisms, which could be the subject of further technological improvements.

On the other hand, our study showed that EDS Maglev trains show particular lateral stability at high speeds, by the use of induced currents in the track and repulsive magnetic forces between the train and rail. This allows for inherent stability without the need for real-time sensing or adjustment. These advantages makes it the forefront of high-speed rail technology nowadays. A notable example of project using EDS is Japan's SCMaglev project, achieving test speeds over 600 km/h. However, for low-speed operations, under the necessary speed for stability, such technology would need auxiliary wheels. Thus, EDS technology is focused for long distance, high speed transports, with the possibility to replace some long-haul flights.

# A

## DERIVATIONS

---

### A.1 EMS

---

#### A.1.1 • DERIVATION OF THE POTENTIAL ENERGY STORED IN THE LEFT GAP BY THE MAGNETIC CIRCUIT METHOD

Here, we find the potential energy stored in the left air gap. Let  $d$  denote the gap between the train and the railway at equilibrium, and  $y$  denote lateral displacement in either direction. Let  $r$  be the radius of the electromagnet. The reluctance of a magnetically uniform magnetic circuit element can be calculated as

$$\mathcal{R} = \frac{l}{\mu A},$$

where  $l$  is the length of the element,  $\mu$  is the permeability of the material and  $A$  is the cross-sectional of the circuit. Since we assumed the permeability of the electromagnet and the railway are high, this yields that the total reluctance of the circuit is given by

$$\mathcal{R}_{total} = \mathcal{R}_{gap},$$

where  $\mathcal{R}_{gap}$  is the reluctance of the two air gaps added together. Yet, if  $h$  denotes the air gap length, this reluctance  $\mathcal{R}_{gap}$  is obtained by

$$\mathcal{R}_{gap} = \frac{2h}{\mu_0 \pi r^2}.$$

Hence:

$$\mathcal{R}_{total} = \frac{2h}{\mu_0 \pi r^2}.$$

In addition, the magnetomotive force  $\mathcal{F}$  in the electromagnet is given by

$$\mathcal{F} = NI,$$

where  $N$  is the number of turns in the electromagnet and  $I$  is the current flowing in the wire. Therefore, by Hopkinson's law, we obtain that the magnetic flux circulating in the magnetic circuit is

$$\Phi = \frac{\mathcal{F}}{\mathcal{R}_{total}} = \frac{\mu_0 \pi r^2 NI}{2h}.$$

Thus the magnitude of the magnetic field is

$$B = \frac{\Phi}{\pi r^2} = \frac{\mu_0 NI}{2h}.$$

Now we want to find the magnetic energy density  $u$  stored in the two air gaps. It is obtained via the equation

$$u = \frac{B^2}{2\mu_0}.$$

Hence:

$$u = \frac{\mu_0 N^2 I^2}{8h^2}.$$

Since the total volume of the air gaps is

$$V = 2\pi r^2 h,$$

we finally obtain that the energy stored is then:

Potential energy stored in the left gap by the magnetic circuit method

$$U_l = uV = \frac{\mu_0 N^2 I^2 \pi r^2}{4h}$$

In particular the force between the electromagnet and the rail is given by:

$$F_l = -\frac{dU_l}{dh} = \frac{\mu_0 N^2 I^2 \pi r^2}{4h^2}.$$

Since on the left side of the rail  $h = d - y$ , this yields:

Force between the electromagnet and the rail

$$F_l(y) = \frac{\mu_0 N^2 I^2 \pi r^2}{4(d - y)^2}.$$

#### A.1.2 • DERIVATION OF THE FORCE EXERTED BY ONE SOURCE COIL ON A TARGET COIL IN THE MAGNETIC DIPOLE APPROXIMATION

Here, we find the force exerted by one source coil of current  $I$  on a target coil of current  $I'$ , both of them being coaxial and separated with distance  $y$ . By symmetry,

$$\vec{B}(y) = B(y)\vec{e}_y.$$

In particular, by Biot-Savart law,

$$\vec{B}(y) = \int_{\Gamma} \frac{I d\vec{l} \times P\vec{M}}{|P\vec{M}|^3},$$

where  $d\vec{l} = r d\theta \vec{e}_{\theta}$  and  $P\vec{M} = (-r)\vec{e}_r + y\vec{e}_y$ . Then,

$$d\vec{l} \times P\vec{M} = \begin{pmatrix} 0 \\ r d\theta \\ 0 \end{pmatrix} \times \begin{pmatrix} -r \\ 0 \\ y \end{pmatrix} = \begin{pmatrix} y r d\theta \\ 0 \\ r^2 d\theta \end{pmatrix} = y r d\theta \vec{e}_r + r^2 d\theta \vec{e}_y.$$

Since  $\vec{B} // \vec{e}_y$ , the term  $y r d\theta \vec{e}_r$  vanishes. We deduce that

$$\vec{B} = \frac{\mu_0 I}{4\pi} \int_{\Gamma} \frac{r^2 d\theta}{(r^2 + y^2)^{3/2}} \vec{e}_y = \frac{\mu_0 I r^2}{4\pi (r^2 + y^2)^{3/2}} \int_{\theta=0}^{\theta=2\pi} d\theta \vec{e}_y = \frac{\mu_0 I}{2} \frac{r^2}{(r^2 + y^2)^{3/2}} \vec{e}_y.$$

Now, to compute magnetic dipole of the target coil of current  $I'$ , we use the formula

$$\vec{m} = I' \vec{S},$$

where  $\vec{S} = \pi r^2 \vec{e}_y$ . Thus,

$$\vec{m} \cdot \vec{B} = \frac{\mu_0 I I' \pi r^4}{2(r^2 + y^2)^{3/2}}.$$

Hence the force exerted by the source coil on the target coil is given by

Force exerted by one source coil of current  $I$  on a target coil of current  $I'$

$$\vec{F} = \vec{\nabla}(\vec{m} \cdot \vec{B}) = -\frac{3}{2} \mu_0 I I' \pi r^4 \frac{y}{(r^2 + y^2)^{5/2}} \vec{e}_y.$$

### A.1.3 • DERIVATION OF THE FORCE EXERTED BY ONE SOURCE COIL ON A TARGET COIL IN SPACE

In this case, we consider that the two coils are not sufficiently far apart to make the dipole moment approximation. However, determining the field generated by a single coil in space without approximations is mathematically demanding, requiring elliptic integrals and long computations. The formulae for the components of the magnetic field generated by a single coil in space were taken from the following article from the Kennedy Space Center<sup>8</sup>. Then, the induced Laplace force was computed numerically in the Python model.

Hence, we base this derivation with the following expression of the magnetic field. In Cartesian coordinates, if  $R$  denotes the radius of the loop and  $I$  the current passing through it, we define the following substitutions:

$$\begin{aligned} C &= \frac{\mu_0 I}{2\pi} \\ \rho_c &= \sqrt{x^2 + y^2} & r_c &= \sqrt{x^2 + y^2 + z^2} \\ \alpha_c &= \sqrt{R^2 + r^2 - 2R\rho} & \beta_c &= \sqrt{R^2 + r^2 + 2R\rho} \\ k &= \sqrt{1 - \frac{\alpha^2}{\beta^2}} & \gamma &= \sqrt{x^2 - y^2} \end{aligned}$$

Then, the coordinates of the magnetic field in our coordinate basis are:

$$\begin{aligned} B_z &= \frac{C}{\alpha_c^2 \beta_c \rho_c^2} xz[(R^2 + r_c^2)E(k^2) - \alpha_c^2 K(k^2)] \\ B_x &= \frac{C}{\alpha_c^2 \beta_c \rho_c^2} yz[(R^2 + r_c^2)E(k^2) - \alpha_c^2 K(k^2)] \\ B_y &= \frac{C}{\alpha_c^2 \beta_c} [(R^2 - r_c^2)E(k^2) + \alpha_c^2 K(k^2)] \end{aligned}$$

In this expression  $K$  and  $E$  denote the complete elliptic integrals of the first and second kinds respectively.

Thanks to this expression, we can deduce the Laplace force generated on a loop in space. In our case, the response loop is identical to the source loop, with same radius, same current, and same orientation along the  $y$ -axis. The latter has center is at distance  $y$  apart along the  $y$ -axis, and at

<sup>8</sup><https://ntrs.nasa.gov/api/citations/20140002333/downloads/20140002333.pdf>

distance  $l$  from the  $y$ -axis. Hence, all the points in the loop can be described in our coordinate basis by:  $(x, y, z) = (\rho \sin \phi, y, \rho \cos \phi)$ . Consider an infinitesimal loop element, i.e. in the form:  $d\vec{l} = (R \cos \phi, 0, -R \sin \phi)d\phi$ . The magnetic field at this point is in particular:  $\vec{B}(R \sin \phi, y, \rho + R \cos \phi) = B_x \vec{e}_x + B_y \vec{e}_y + B_z \vec{e}_z$ . We deduce that

$$d\vec{l} \times \vec{B} = (-B_y R \sin \phi \vec{e}_y - (B_x R \sin \phi + B_z R \cos \phi) \vec{e}_y + B_y R \cos \phi \vec{e}_z) d\phi$$

and in particular, we can use  $d\vec{F}_{Laplace} = I d\vec{l} \times \vec{B}$  to compute  $\vec{F}_{Laplace}$ . Since only the guidance force, along the  $y$ -axis, is of interest, we only compute:

$$F_y(\rho, y) = -IR \int_{\phi=0}^{2\pi} (B_x \sin \phi + B_z \cos \phi) d\phi$$

To take into account multiple loops superposed at the same point, we would need to multiply both the field and the force by the number of coils. In our model, this number was  $\frac{N}{2}$ , changing the force to:

Force exerted by one source coil on a target coil in space

$$F_y(\rho, y) = -IR \frac{N^2}{4} \int_{\phi=0}^{2\pi} (B_x \sin \phi + B_z \cos \phi) d\phi.$$

## A.2 EDS

### A.2.1 • DERIVATION OF THE FLUX AND CURRENT

We would like to detail all of our analytical derivations throughout the paper, which were summarized in the first sections but not detailed. We first derive the magnetic flux over one entier 8-shape coil by one train coil. We remind:

- $R$ : radius of train coils
- $R_{\text{guide}}$ : radius of guideway loops
- $x_h = (2h - 1)R$ : position of train coil  $h$
- $x_j = (2j - 1)R_{\text{guide}}$ : horizontal position of guideway loop  $j$
- $y_{\text{side}} = \pm \frac{L}{2}$ : lateral position (right: +, left: -)
- $z_{\text{loop}} = z_0 \pm R_{\text{guide}}$ : vertical position (top: +, bottom: -)
- $z_1$ : vertical position of train coils
- $y$ : lateral position of train (variable)
- $\mathbf{r} = \begin{pmatrix} X \\ Y \\ Z \end{pmatrix} = \begin{pmatrix} x_j - x_h \\ \pm \frac{L}{2} - y \\ z_0 \pm R_{\text{guide}} - z_1 \end{pmatrix}$ : relative position vector from the train coil to the loop
- $\mathbf{M}_h = (-1)^h I \pi R^2 \mathbf{e}_y$

B-field at guideway coil center from train coil h

$$\begin{aligned}\mathbf{B}(\mathbf{r}) &= \frac{\mu_0}{4\pi} \frac{3(\mathbf{M}_h \cdot \mathbf{r})\mathbf{r} - \mathbf{M}_h r^2}{r^5} \\ &= \frac{\mu_0 M_h}{4\pi} \frac{3Y\mathbf{r} - \mathbf{e}_y r^2}{r^5}\end{aligned}$$

The only component of  $\mathbf{B}$  which interests us is the  $y$  component due to the dot product with  $d\mathbf{S}$  in the flux, which is along  $\mathbf{e}_y$

B-field at guideway coil center from train coil h

$$B_y(\mathbf{r}) = \frac{\mu_0 M_h}{4\pi} \frac{3Y^2 - r^2}{r^5}$$

Then, with our assumption that the B-field of the train coils is uniform over any guideway coil, we get that:

Flux in one guideway coil from train coil h

$$\begin{aligned}\Phi_{h,j}^{\text{side,loop}} &= \int_S \mathbf{B} \cdot d\mathbf{S} = \mathbf{B}(\mathbf{r}) \pi R_{\text{guide}}^2 \\ &= \frac{\mu_0 M_h R_{\text{guide}}^2}{4} \frac{3Y^2 - r^2}{r^5}\end{aligned}$$

Now define:

$$r_{\pm}^2 = X^2 + Y^2 + (z_0 \pm R_{\text{guide}} - z_1)^2$$

This gives the flux in an 8-shape coil from a single train coil:

Flux in an 8-shape coil from train coil h

$$\begin{aligned}\Phi_{h,j}^{\text{side}} &= \Phi_{h,j}^{\text{side,top}} - \Phi_{h,j}^{\text{side,bottom}} \\ &= \frac{\mu_0 M_h R_{\text{guide}}^2}{4} \left[ \frac{3Y^2 - r_+^2}{r_+^5} - \frac{3Y^2 - r_-^2}{r_-^5} \right]\end{aligned}$$

Having this, we can compute the total flux in an 8-shape coil. Due to the principle of superposition, the total flux over one 8-shape coil is the sum of the flux from each of the train coils (all 4 of them). We then have:

Flux in an 8-shape coil from all 4 train coils

$$\begin{aligned}\Phi_j^{\text{side}} &= \sum_{h=1}^4 \Phi_{h,j}^{\text{side,top}} - \Phi_{h,j}^{\text{side,bottom}} \\ &= \sum_{h=1}^4 \frac{\mu_0 M_h R_{\text{guide}}^2}{4} \left[ \frac{3Y^2 - r_+^2}{r_+^5} - \frac{3Y^2 - r_-^2}{r_-^5} \right]\end{aligned}$$

Important: We remind that  $r_+$  and  $r_-$  also depend on  $h$ , as  $X$  depends on  $h$ .

This expression captures the net flux contribution of all 4 train train dipoles to a given figure-8



guideway coil and will be used in the computation of the induced magnetic moments in the guideway coils.

We now want to derive this expression with respect to time to obtain the current through one 8-shap coil.

#### Deriving the current $i$ through an 8-shape coil

$$i_j^{\text{side}}(t) = -\frac{1}{R_E} \cdot \frac{d}{dt} (\Phi_j^{\text{side}}(t))$$

$$\frac{d}{dt}(\Phi) = \frac{d\Phi}{dX} \cdot \frac{dX}{dt} = -v \cdot \frac{d\Phi}{dX} \Rightarrow i_j^{\text{side}}(t) = \frac{v}{R_E} \cdot \frac{d}{dX} (\Phi_j^{\text{side}}(X))$$

We have:  $\frac{d}{dX} \left( \frac{3Y^2 - r_{\pm}^2}{r_{\pm}^5} \right) = \frac{-2X}{r_{\pm}^5} + \frac{5X(3Y^2 - r_{\pm}^2)}{r_{\pm}^7}$

$$\Rightarrow \frac{d\Phi_j^{\text{side}}(t)}{dX} = \sum_{h=1}^4 \frac{\mu_0 M_h R_{\text{guide}}^2}{4} \left[ \left( \frac{-2X}{r_+^5} + \frac{5X(3Y^2 - r_+^2)}{r_+^7} \right) - \left( \frac{-2X}{r_-^5} + \frac{5X(3Y^2 - r_-^2)}{r_-^7} \right) \right]$$

This gives us the final formula for the current through one 8-shap coil:

#### Induced current through an 8-shape coil due to one train coil

$$i_j^{\text{side}}(t) = \sum_{h=1}^4 \frac{v \mu_0 M_h R_{\text{guide}}^2}{4 R_E} \left[ \left( \frac{-2X}{r_+^5} + \frac{5X(3Y^2 - r_+^2)}{r_+^7} \right) - \left( \frac{-2X}{r_-^5} + \frac{5X(3Y^2 - r_-^2)}{r_-^7} \right) \right]$$

Having the current now allows us to deduce the induced magnetic field, and derive the potential energy felt by the train.

### A.2.2 • DERIVATION OF THE MAGNETIC FIELD AND POTENTIAL ENERGY

Each figure-8 guideway coil consists of a top and bottom circular loop of radius  $R_{\text{guide}}$ , carrying the same induced current  $i_j^{\text{side}}(t)$  as derived previously. Due to their opposite winding directions, the magnetic dipole moments of the two loops point in opposite directions. In this section, we compute the magnetic field produced by each loop separately at the position of a train coil, then sum their contributions.

We go back to the definition of a magnetic dipole moment and use the fact that:

$$\mathbf{m} = i \cdot \pi R_{\text{guide}}^2 \cdot \mathbf{n}$$

In the case of our 8-shape coil, we have:

### Opposing dipole moments for one 8-shape coil

$$\begin{aligned}\mathbf{m}_j^{\text{side,top}}(t) &= +i_j^{\text{side}}(t) \cdot \pi R_{\text{guide}}^2 \cdot \mathbf{e}_y \\ \mathbf{m}_j^{\text{side,bottom}}(t) &= -i_j^{\text{side}}(t) \cdot \pi R_{\text{guide}}^2 \cdot \mathbf{e}_y\end{aligned}$$

We now want to determine the B-field from the guideway coils on to the train coils, in order to determine the potential energy. For this, we need to define a new relative position vector. In reality, this vector is nearly the same as the one for the first section, with reversed signs. But let us be especially clear about which coil we take into account. We remind:

- $x_p = (2p - 1)R$ : position of train coil  $p$
- $x_j = (2j - 1)R_{\text{guide}}$ : horizontal position of guideway loop  $j$
- $y_{\text{side}} = \pm \frac{L}{2}$ : lateral position (right: +, left: -)
- $z_{\text{loop}} = z_0 \pm R_{\text{guide}}$ : vertical position (top: +, bottom: -)
- $z_1$ : vertical position of train coils
- $y$ : lateral position of train (variable)

We define two new position vectors:

$$\begin{aligned}\mathbf{r}^{\text{top}} &= \begin{pmatrix} X' \\ Y' \\ Z' - R_{\text{guide}} \end{pmatrix} = \begin{pmatrix} x_p - x_j \\ y - y_j \\ z_1 - z_0 - R_{\text{guide}} \end{pmatrix}, \quad r_{\text{top}}^2 = X'^2 + Y'^2 + (Z' - R_{\text{guide}})^2 \\ \mathbf{r}^{\text{bottom}} &= \begin{pmatrix} X' \\ Y' \\ Z' + R_{\text{guide}} \end{pmatrix} = \begin{pmatrix} x_p - x_j \\ y - y_j \\ z_1 - z_0 + R_{\text{guide}} \end{pmatrix}, \quad r_{\text{bottom}}^2 = X'^2 + Y'^2 + (Z' + R_{\text{guide}})^2\end{aligned}$$

We are now ready to compute the induced B-field. Recall the formula of the magnetic field generated by a dipole of moment  $\mathbf{m}$ :

$$\mathbf{B}(\mathbf{r}) = \frac{\mu_0}{4\pi r^5} [3(\mathbf{m} \cdot \mathbf{r})\mathbf{r} - r^2\mathbf{m}]$$

We separate the contributions from the top and bottom loops:

### Magnetic field from the top loop onto train coil $p$

$$\begin{aligned}\mathbf{B}_{p,j}^{\text{side,top}}(\mathbf{r}_{\text{top}}, t) &= \frac{\mu_0}{4\pi r_{\text{top}}^5} [3(\mathbf{m}_j^{\text{side,top}} \cdot \mathbf{r}^{\text{top}})\mathbf{r}^{\text{top}} - r_{\text{top}}^2\mathbf{m}_j^{\text{side,top}}] \\ &= \frac{\mu_0 m_j^{\text{side,top}}(t)}{4\pi (r_{\text{top}}^2)^{5/2}} [3Y'\mathbf{r}^{\text{top}} - r_{\text{top}}^2\mathbf{e}_y]\end{aligned}$$

### Magnetic field from the bottom loop onto train coil $p$

$$\begin{aligned}\mathbf{B}_{p,j}^{\text{side,bottom}}(\mathbf{r}_{\text{bottom}}, t) &= \frac{\mu_0}{4\pi r_{\text{bottom}}^5} [3(\mathbf{m}_j^{\text{side,bottom}} \cdot \mathbf{r}^{\text{bottom}})\mathbf{r}^{\text{bottom}} - r_{\text{bottom}}^2\mathbf{m}_j^{\text{side,bottom}}] \\ &= \frac{\mu_0 m_j^{\text{side,bottom}}(t)}{4\pi (r_{\text{bottom}}^2)^{5/2}} [3Y'\mathbf{r}^{\text{bottom}} - r_{\text{bottom}}^2\mathbf{e}_y]\end{aligned}$$

We can now deduce the total field from one 8-shape loop felt by train coil  $p$ :

Magnetic field from an 8-shape coil onto train coil  $p$

$$\mathbf{B}_{j,p}^{\text{side}}(t) = \mathbf{B}_{j,p}^{\text{side,top}}(t) + \mathbf{B}_{j,p}^{\text{side,bottom}}(t)$$

We are now able to derive the magnetic potential energy upon train coil  $p$  using that the magnetic potential energy of a magnetic dipole  $\mathbf{M}$  in a magnetic field  $\mathbf{B}$  is given by:

$$U = -\mathbf{M} \cdot \mathbf{B}$$

Since for all the train coils, the magnetic dipole moment  $\mathbf{M}_p$  is along  $\mathbf{e}_y$ , we are only interested in the  $\mathbf{e}_y$  component of the B-field. Let us compute this component explicitly:

$y$ -component of the magnetic field from an 8-shape coil onto train coil  $p$

$$\begin{aligned} B_{j,p}^{\text{side}}(t)_y &= B_{j,p}^{\text{side,top}}(t)_y + B_{j,p}^{\text{side,bottom}}(t)_y \\ &= \frac{\mu_0 m_j^{\text{side,top}}(t)}{4\pi(r_{\text{top}}^2)^{5/2}} [3Y'^2 - r_{\text{top}}^2] + \frac{\mu_0 m_j^{\text{side,bottom}}(t)}{4\pi(r_{\text{bottom}}^2)^{5/2}} [3Y'^2 - r_{\text{bottom}}^2] \end{aligned}$$

We can now express the potential energy felt by one train coil from the guideway coils considered:

Potential energy of one train coil

$$U(t, y)_p = -M_p \sum_{\text{side} \in \{\text{left}, \text{right}\}} \sum_{j=1}^2 \left( B_{j,p}^{\text{side,top}}(t, y)_y + B_{j,p}^{\text{side,bottom}}(t, y)_y \right)$$

Now, we can derive the potential energy of the whole train simply by summing over the train coils:

Potential energy of the whole train

$$U(t, y) = - \sum_{p=1}^4 M_p \sum_{\text{side} \in \{\text{left}, \text{right}\}} \sum_{j=1}^2 \left( B_{j,p}^{\text{side,top}}(t, y)_y + B_{j,p}^{\text{side,bottom}}(t, y)_y \right)$$

## B

# SIMULATION CODE

---

### B.1 EMS

---

#### B.1.1 • PYTHON CODE FOR THE SIMULATION USING THE MAGNETIC CIRCUIT METHOD

```

1 import numpy as np
2 import matplotlib.pyplot as plt
3 import scipy.integrate as integrate
4 from scipy.integrate import cumtrapz
5
6 # Physical constants / parameters (example values)
7 mu0 = 4 * np.pi * 1e-7 # Vacuum permeability [H/m]
8 I = 57.0 # Current of coil A [A]
9 alph = 1.0 # Current of coil B [A] is alph*I
10 R = 0.06 # Radius [m]
11 d = 0.011 # Distance parameter [m]
12 N = 210 # Number of coils
13 A = np.pi * R**2
14
15
16 def F(dist):
17     return (mu0 * A * N**2)/4 * (I/dist)**2
18
19
20 # Composite forces
21 def FA(x):
22     return F(d - x)
23
24 def FB(x):
25     return -alph**2 * F(d + x)
26
27 def Ft(x):
28     return FA(x) + FB(x)
29
30 # Set up x grid
31 x_vals = np.linspace(-d+d/10, d-d/10, 1000)
32
33 # Compute on that grid
34 F_vals = Ft(x_vals)
35 FA_vals = FA(x_vals)
36 FB_vals = FB(x_vals)
37
38 # Numerically integrate -F to get U, with U(-d)=0
39 U_vals = np.concatenate(([0], cumtrapz(-F_vals, x_vals)))
40
41 # Plot F, FA, FB
42 plt.figure(figsize=(10,4))
43
44 plt.subplot(2,1,1)
45 plt.plot(x_vals, F_vals, label='F(x)')
```

```

46 plt.plot(x_vals, FA_vals, '--', label='F_A(x)')
47 plt.plot(x_vals, FB_vals, '--', label='F_B(x)')
48 plt.axhline(0, color='gray', ls='--', lw=0.5)
49 plt.xlabel('Lateral displacement y (m)')
50 plt.ylabel('Force (N)')
51 plt.title('Forces vs. lateral displacement')
52 plt.legend()
53 plt.grid(True)
54
55 # Plot U(x)
56 plt.subplot(2,1,2)
57 plt.plot(x_vals, U_vals)
58 plt.xlabel('Lateral displacement y (m)')
59 plt.ylabel('Potential energy U (J)')
60 plt.title('Potential energy vs. lateral displacement')
61 plt.grid(True)
62
63 plt.tight_layout()
64 plt.show()

```

### B.1.2 • PYTHON CODE FOR THE SIMULATION WITH ONE COIL PER ELECTROMAGNET USING THE METHOD OF IMAGES

```

1 import numpy as np
2 import matplotlib.pyplot as plt
3 from scipy.integrate import cumtrapz
4
5 # Physical constants / parameters (example values)
6 mu0 = 4 * np.pi * 1e-7 # Vacuum permeability [H/m]
7 I = 57.0 # Current [A]
8 alph = 1.0 # Current ratio
9 IA = I # Current of coil A [A]
10 IB = alph*I # Current of coil B [A]
11 R = 0.002 # Radius [m]
12 d = 0.011 # Air gap [m]
13 L = 4.0 # Width of the guideway [m]
14
15 # Define f(z)
16 def f(z):
17     return z / (R**2 + z**2)**(5/2)
18
19 # Define FA(x) and FB(x)
20 def FA(x):
21     return (3 * mu0 * IA * np.pi * R**4 / 2) * (
22         IA * f(2*d - 2*x) + IB * f(L + 2*d) + IB * f(L - 2*x)
23     )
24
25 def FB(x):
26     return -(3 * mu0 * IB * np.pi * R**4 / 2) * (
27         IB * f(2*d + 2*x) + IA * f(L + 2*d) + IA * f(L + 2*x)
28     )
29
30 # Define F(x)
31 def F(x):
32     return FA(x)+FB(x)

```

```

33
34 # Set up x grid
35 x_vals = np.linspace(-d, d, 1000)
36
37 # Compute F, FA, FB on that grid
38 F_vals = F(x_vals)
39 FA_vals = FA(x_vals)
40 FB_vals = FB(x_vals)
41
42 # Numerically integrate -F to get U, with U(-d) = 0
43 U_vals = np.concatenate(([0], cumtrapz(-F_vals, x_vals)))
44
45 # Plot F, F1, F2
46 plt.figure(figsize=(10,4))
47
48 plt.subplot(2,1,1)
49 plt.plot(x_vals, F_vals, color='blue', label='Total force F(x)')
50 plt.plot(x_vals, FA_vals, ':', color='orange', label='Left force FA(x)')
51 plt.plot(x_vals, FB_vals, ':', color='magenta', label='Right force FB(x)')
52 plt.axhline(0, color='gray', ls='--', linewidth=0.5)
53 plt.xlabel('Lateral displacement y (m)')
54 plt.ylabel('Force F (N)')
55 plt.title('Lateral forces as a function of the lateral displacement')
56 plt.legend()
57 plt.grid(True)
58
59 # Plot U(x)
60 plt.subplot(2,1,2)
61 plt.plot(x_vals, U_vals)
62 plt.xlabel('Lateral displacement y (m)')
63 plt.ylabel('Potential energy (J)')
64 plt.title('Potential energy as a function of lateral displacement')
65 plt.grid(True)
66
67 plt.tight_layout()
68 plt.show()

```

### B.1.3 • PYTHON CODE FOR THE SIMULATION WITH TWO COILS OF OPPOSITE CURRENT PER ELECTROMAGNET USING THE METHOD OF IMAGES

```

1
2 import numpy as np
3 import matplotlib.pyplot as plt
4 from scipy.integrate import cumtrapz
5 import scipy.integrate as integrate
6
7 from scipy.special import ellipk, ellipe, ellipkm1
8 from numpy import pi, sqrt, linspace
9 from pylab import plot, xlabel, ylabel, suptitle, legend, show
10
11 muo = 4E-7*pi
12 I     = 57.0           # Current of coil A [A]
13 alph  = 1.0           # Current of coil B [A] is alph*I
14 R     = 0.06          # Radius of coils [m]
15 A     = np.pi * R**2 # Cross-section area [m^2]

```

```

16 d      = 0.011          # Air gap [m]
17 L      = 4.0            # Rail length [m]
18 N      = 210            # Number of coils
19 l      = 0.2            # Solenoid length [m]
20 n      = N / L
21
22 C = lambda I: muo*I/pi
23 rho = lambda x, y: x**2+y**2
24 rad = lambda x, y, z: x**2+y**2+z**2
25 al = lambda x, y, z: R**2+rad(x,y,z)**2-2*R*rho(x,y)
26 bt = lambda x, y, z: R**2+rad(x,y,z)**2+2*R*rho(x,y)
27 k = lambda x, y, z: 1 - al(x,y,z)/bt(x,y,z)
28 gam = lambda x, y: x**2 - y**2
29 K = lambda x, y, z: ellipk(k(x,y,z))
30 E = lambda x, y, z: ellipse(k(x,y,z))
31 const = lambda x, y, z: C(I)/(2*al(x,y,z)*bt(x,y,z)**0.5)
32 exprr = lambda x, y, z: (R**2+rad(x,y,z))*E(x,y,z) - al(x,y,z)*K(x,y,z)
33
34
35 def Bx(x, y, z):
36     return N/2 * const(x,y,z)*x*z/rho(x,y) * exprr(x,y,z)
37
38 def By(x, y, z):
39     return N/2 * const(x,y,z)*y*z/rho(x,y) * exprr(x,y,z)
40
41 def Bz(x, y, z):
42     return N/2 * const(x,y,z)*((R**2-rad(x,y,z))*E(x,y,z) + al(x,y,z)*K(x,y,z))
43
44 def dF(rr, z, th):
45     return -R * I * N/2 * (Bx(rr+R*np.cos(th), R*np.sin(th), z)*np.cos(th) + By(rr+R*
46         np.cos(th), R*np.sin(th), z)*np.sin(th))
47
48 def Fo(z):
49     integ, err = integrate.quad(lambda th: dF(0, z, th), 0, 2*np.pi)
50     return integ
51
52 def Fl(z):
53     integ, err = integrate.quad(lambda th: dF(l, z, th), 0, 2*np.pi)
54     return integ
55
56 def res(z):
57     return (Fo(z) - Fl(z))
58
59 def FA(y):
60     return 2*res(2*d-2*y)
61
62 def FB(y):
63     return -alph**2 * 2*res(2*d+2*y)
64
65 def F(y):
66     return FA(y) + FB(y)
67
68 x_vals = np.linspace(-d+d/20, d-d/20, 1000)
69
70 FA_vals = np.array([FA(i) for i in x_vals])
71 FB_vals = np.array([FB(i) for i in x_vals])
72 F_vals = np.array([F(i) for i in x_vals])

```



```

72
73 U_vals = np.concatenate(([0], cumtrapz(-F_vals, x_vals)))
74
75 plt.figure(figsize=(10,4))
76
77 plt.subplot(2,1,1)
78 plt.plot(x_vals, F_vals, color='blue', label='Total force F(x)')
79 plt.plot(x_vals, FA_vals, ':', color='orange', label='Left force FA(x)')
80 plt.plot(x_vals, FB_vals, ':', color='magenta', label='Right force FB(x)')
81 plt.axhline(0, color='gray', ls='--', linewidth=0.5)
82 plt.xlabel('Lateral displacement y (m)')
83 plt.ylabel('Force (N)')
84 plt.title('Lateral forces as a function of the lateral displacement')
85 plt.legend()
86 plt.grid(True)
87
88 # Plot U(x)
89 plt.subplot(2,1,2)
90 plt.plot(x_vals, U_vals)
91 plt.xlabel('Lateral displacement y (m)')
92 plt.ylabel('Potential energy U (J)')
93 plt.title('Potential Energy as a function of lateral displacement')
94 plt.grid(True)
95
96 plt.tight_layout()
97 plt.show()

```

## B.2 EDS

### B.2.1 • DEFINITION OF THE PARAMETERS

```

1
2 # Parameters of the actual nature.
3 mu0 = 4 * np.pi * 1e-7
4 Res = 10
5
6 I = 700000
7 R_g = 1
8 R_c = 1.5 #Train coils I believe...
9 A_g = 3.14 * (R_g)**2
10 n = 2 #Number of guide coils that the train sees
11
12
13 M = (R_c**2) * np.pi * I
14
15 L = 1.2
16 z_0 = 0.7 #The closer to the center, the better it is.
17 x_vt = 30 # assume x(vt) = 0 for plotting

```

### B.2.2 • DEFINING THE TIME-DERIVATIVE AND CURRENT ON AN 8-COIL LOOP

```

1 """

```

```

2 We are interested in what the guideway coil sees as the train passes through it.
3   - Fix the guideway's 8-coil center at  $x = 0$ ,  $z_{up} = + R_g$ ,  $y = L/2$ 
4   - And, we want the format of the flux through time.
5   - We want to establish the flux through time of the guidecoil, then differentiate
    it.
6   - We desire a graph for flux(debug) and current through time
7   """
8 def r_train(h, t, y_train):
9     #The idea is that each of the train's coil's position can be parameterized with
    only h and t.
10    output = []
11    output.append(x_vt*t + 2 * (h-1) * R_c)
12    #print(x_vt*t + 2 * (h-1) * R_c)
13    output.append(y_train) #This is not a constant!!! Defined per function...
14    output.append(z_0)
15    #returns the x, y, z of the train.
16    return output
17
18 def r_squared_func(xg, yg, zg, h, t, y):
19     #A helper function that computes for every train coil's distance to a specific
    guide coil at position x, y, z
20    [xt, yt, zt] = r_train(h, t, y) #! the t is not fixed
21    return (xg - xt)**2 + (yg - yt)**2 + (zg - zt)**2
22
23 def flux(x, y, z, t, lr, y_train = 0):
24     #Flux centered at a certain position x, y, z for the center of the coil.
25     #Therefore, the position of the train is determined already and is ran through
    system.
26    total = 0
27    for h in range(1, 5): # h = 1 to 4
28        sign = (-1)**h
29        r_squared = r_squared_func(x, y, z, h, t, y_train)
30        r_five = max(r_squared * (2.5), 1e-10)
31        numerator = 3 * (y_train - (-1)**lr * L/2)**2 - r_squared
32        term = (mu0 * sign * M * R_g**2 / 4) * (numerator / r_five)
33        total += term
34    #print(total)
35    return total
36
37 def eight_coil_flux(xg, yg, zg, t, lr, y_train = 0):
38     return flux(xg, yg, R_g, t, y_train, lr) + flux(xg, yg, 0 - R_g, t, y_train, lr)
39
40 def emf(x, y, z, t, lr, y_train = 0):
41     h = 1e-5
42     return (eight_coil_flux(x, y, z, t + h, y_train, lr) - eight_coil_flux(x, y, z, t
    - h, y_train, lr)) / (2 * h)
43
44 #Application for generating graphs:
45 t_vals = np.linspace(2.6, 3.1, 500)
46 x_coil = 90
47 flux_vals = np.array([eight_coil_flux(x_coil, L/2, R_g, t, 0) for t in t_vals])
48 lr = 1 #This comes into importance in the B-field section
49 dflux_vals = np.array([emf(x_coil, L/2, R_g, t, 1, 0) for t in t_vals])
50 dflux_vals = (1/Res) * dflux_vals
51
52
53 #Analysis using FFT

```

```

54 def compute_fft(signal, t_vals):
55     """
56     Computes the FFT of a signal and returns frequency and amplitude spectrum.
57     """
58     n = len(signal)
59     dt = float(t_vals[1] - t_vals[0]) # time step
60     freqs = jnp.fft.fftfreq(n, d=dt)   # frequency bins
61     fft_vals = jnp.fft.fft(signal)     # complex FFT values
62     amplitude = jnp.abs(fft_vals) / n # normalize amplitude
63
64     # Only keep the positive half of the spectrum
65     half_n = n // 2
66     return freqs[:half_n], amplitude[:half_n]
67
68 # --- Compute and Plot FFT ---
69 freqs, amp = compute_fft(dflux_vals, t_vals)
70 peak_idx = np.argmax(amp)
71 peak_freq = freqs[peak_idx]
72 print(peak_freq)

```

### B.2.3 • COMPUTING THE B-FIELD ALONG ONE SLICE OF THE GUIDEWAY AND POTENTIAL

```

1 #The current and the other thing that is useful is the emf function given from above.
  There will be the same current through the entire 8-coil.
2 #From this 8-coil current, we expect to see an essentially equal field on all four
  corners
3 #This part will intergrate and vary the position y of the train aforesaid within
  the functions. Currently, only the flux has such a dependence.
4
5 def current(y_train, lr, x_coil, t):
6     # Computes induced current in a guideway 8-coil loop at time
7     y_loop = ((-1)**lr) * (L / 2)
8     phi_dot = emf(x_coil, y_loop, R_g, t, lr, y_train)
9     phi_dot = phi_dot / Res
10    return phi_dot
11 #The consequence of noting it as such is that we simplifie that there are only two
  guide coils to consider.
12
13 def B_field(x, y, z, t, y_train, x_coil=x_coil):
14     """
15     Computes the y-component of the magnetic field at (x, y, z)
16     due to ONE guideway coil at x_coil, side lr, with current induced by train at
17     y_train.
18
19     Parameters:
20     - x, y, z: Field evaluation point
21     - t: Time (s)
22     - y_train: Train's lateral position
23     - x_coil: x-position of the guideway coil (default = 0)
24     - lr: 1 for right (+L/2), 2 for left (-L/2)
25
26     Returns:
27     - B_y: y-component of the magnetic field at (x, y, z) from 1 eight_coil.
28     """
29     total_B = 0
30     for lr in [1, 2]: #Sum the left and right eight-coils

```

```

30     y_coil = ((-1)**lr) * (L / 2) #The position of the 8-coil...
31
32     for loop_sign in [+1, -1]: #The up and the down of the eight-coil.
33         z_coil = loop_sign * R_g
34
35         # Compute relative position vector
36         dx = x - x_coil
37         dy = y - y_coil
38         dz = z - z_coil
39         r_vec = np.array([dx, dy, dz])
40         r_squared = np.dot(r_vec, r_vec)
41
42         r_five = r_squared**5
43         r_five = np.sqrt(r_five)
44
45         # Magnetic moment (loop_sign handles top/bottom coil contribution)
46         I_loop = current(y_train, lr, x_coil, t) #This SHOULD be the same current
47         for the up and for the down.
48         M = loop_sign * I_loop * np.pi * R_g**2
49         M_vec = np.array([0, M, 0])
50         M_dot_r = np.dot(M_vec, r_vec)
51
52         # Magnetic field from dipole
53         B_vec = (mu0 / (4 * np.pi)) * ((3 * M_dot_r * r_vec - M_vec * r_squared)
54         / r_five)
55         total_B += (B_vec[1])
56
57     # Return only y-component
58     return total_B
59 def compute_potential(y_train, t, M=M):
60
61     x = x_coil - 0.28 #IMPORTANT, in the development, this was seen as an optional,
62     but due to the degree of freedom on the guidance position, we use this to see the
63     B-field close to a single B-field. This was chosen as we are considering fields
64     between the guidecoils, which is arbitrarily seen as around a third of its radius
65     z = z_0 #height of the train...
66
67     B_y = B_field(x, y_train, z, t, y_train, x_coil=x_coil)
68
69     # Magnetic potential energy: U = -M      B, with M along y-direction
70     U = - M * B_y
71     return U
72
73 def compute_average_potential(y_train, t_vals):
74     U_vals = [compute_potential(y_train, t) for t in t_vals]
75     return np.mean(U_vals)
76
77 \
78
79 1
80 2
81 3 U_vals = np.array([compute_potential(y_train_fixed, t) for t in t_vals])
82 4
83 5 def find_hump_duration(t_vals, U_vals, threshold_ratio=0.05): #Just trust chatgpt on
84     this one, I doubt the precision is all that important.
85     """
86     Finds the duration of the 'hump' in potential energy.

```

```

8
9 Parameters:
10     t_vals: array of time values
11     U_vals: array of potential energy values
12     threshold_ratio: fraction of the max(abs(U_vals)) to define signal bounds
13
14 Returns:
15     t_start, t_end, duration
16 """
17 U_abs = np.abs(U_vals)
18 threshold = threshold_ratio * np.max(U_abs)
19
20 # Find where signal exceeds threshold
21 significant_indices = np.where(U_abs > threshold)[0]
22
23 if len(significant_indices) == 0:
24     return None, None, 0 # No hump found
25
26 start_index = significant_indices[0]
27 end_index = significant_indices[-1]
28
29 t_start = t_vals[start_index]
30 t_end = t_vals[end_index]
31 duration = t_end - t_start
32
33 return t_start, t_end, duration
34
35 t_start, t_end, duration = find_hump_duration(t_vals, U_vals)

```

## B.2.4 • FINAL PLOTTING

```

1
2 def plot_average_potential_vs_y(y_min=-4, y_max=4, y_step=0.05, t_start=0, t_end=1,
3     num_t_points=400):
4     """
5     Plots the time-averaged potential energy of the train as a function of lateral
6     displacement y.
7
8     Parameters:
9     - y_min, y_max: Range of y positions to evaluate (m)
10    - y_step: Step size for y (m)
11    - t_start, t_end: Time interval for averaging (s)
12    - num_t_points: Number of time samples
13    """
14    y_vals = np.arange(y_min, y_max + y_step, y_step)
15    t_vals = np.linspace(t_start, t_end, num_t_points)
16
17    U_avg_vals = [compute_average_potential(y, t_vals) for y in y_vals]
18    U_avg_vals = np.array(U_avg_vals)
19    U_avg_vals -= U_avg_vals.min() # shift so minimum is at zero
20
21    plt.figure(figsize=(10, 6))
22    plt.plot(y_vals, U_avg_vals, color='darkgreen', label='Time-averaged U(y)')
23    plt.xlabel('Lateral position y (m)')
24    plt.ylabel('Time-averaged Potential Energy U(y) (J)')

```

```
24 plt.axvline(x=-L/2, color='red', linestyle='--', label=r'Left coil')
25 plt.axvline(x= L/2, color='red', linestyle='--', label=r'Right coil')
26
27 plt.title('Time-Averaged Magnetic Potential Energy over a period along lateral
28 axis y, v = 30m/s')
29 plt.grid(True)
30 plt.legend()
31 plt.tight_layout()
32 plt.show()
33 #plot_average_potential_vs_y(t_start=t_start, t_end=t_end) #This is defined in the
34 #cell that calculates the duration of the train's traversal.
35 plot_average_potential_vs_y(t_start=t_start, t_end=t_start + period) #On a single
36 period.
```

## C REFERENCES

---

### On ResearchGate:

- <https://www.researchgate.net/publication/37421972>
- <https://www.researchgate.net/publication/269855273>
- <https://www.researchgate.net/publication/329565491>

### On ScienceDirect:

- <https://www.sciencedirect.com/science/article/pii/S0307904X21002080>
- <https://www.sciencedirect.com/science/article/pii/S0141029617339020>
- <https://www.sciencedirect.com/science/article/pii/S0921453425000383>

### On Springer:

- <https://link.springer.com/article/10.1007/s40864-019-0104-1>

### On other libraries:

- <https://ieeexplore.ieee.org/stamp/stamp.jsp?tp=&arnumber=1644911>
- <https://ieeexplore.ieee.org/stamp/stamp.jsp?tp=&arnumber=4376586>
- <https://www.mdpi.com/1996-1073/16/7/2995>
- <https://www.mdpi.com/2076-0825/13/8/314>
- [https://library.acadlore.com/MITS/2023/2/1/MITS\\_02.01\\_05.pdf](https://library.acadlore.com/MITS/2023/2/1/MITS_02.01_05.pdf)

### Miscellaneous articles:

- <https://ntrs.nasa.gov/api/citations/20140002333/downloads/20140002333.pdf>
- <https://koreascience.kr/article/JAKO201709641401416.pdf>
- <https://dspace.mit.edu/handle/1721.1/16351>
- <https://www.emworks.com/en/application/optimizing-magnetic-levitation-for-semi-high-speed-maglev-trains>
- [http://maglev.ir/eng/documents/papers/journals/IMT\\_JP\\_34.pdf](http://maglev.ir/eng/documents/papers/journals/IMT_JP_34.pdf)